J. Fluid Mech. (1993), vol. 355, pp. 129–156

Taylor dispersion of orientable Brownian particles in unbounded homogeneous shear flows

By I. FRANKEL[1] AND H. BRENNER[2]

[1] Faculty of Aerospace Engineering, Technion – Israel Institute of Technology, Haifa 32000, Israel

[2] Department of Chemical Engineering, Massachusetts Institute of Technology, Cambridge, MA 02139, USA

(Received 2 January 1992 and in revised form 5 April 1993)

The physical- and orientation-space transport of *non-spherical*, generally non-neutrally buoyant, Brownian particles in unbounded homogeneous shear flows is analysed with the goal of studying the respective effects of the orientational degrees of freedom of such particles upon their sedimentation and dispersion rates. In particular, the present contribution concentrates on the interaction between the Taylor dispersion mechanism (arising from coupling between the orientational dependence of the particle's translational velocity and the stochastic sampling of the orientation space via rotary Brownian diffusion) and the shear velocity field.

Making use of a recent extension of generalized Taylor dispersion theory to homogeneous (unbounded) shear flows, the mean transport process in physical space is modelled by a convection–diffusion problem characterized by a pair of *constant* phenomenological coefficients, provided that the eigenvalues of the (constant) undisturbed velocity gradient are purely imaginary. The latter phenomenological coefficients – namely, $\boldsymbol{U}^*$, the average 'slip velocity' vector (of the particles relative to the ambient fluid), and $\boldsymbol{D}^*$, the dispersivity dyadic or, equivalently, the pair of dyadics $\bar{\boldsymbol{M}}$ and $\boldsymbol{D}^C$ (or $\bar{\boldsymbol{D}}^C$), the average mobility and the Taylor (or modified Taylor) dispersivity, respectively – are evaluated both asymptotically (in the respective limits of small and large rotary Peclét numbers) as well as numerically (for arbitrary Peclét numbers).

It is established that (up to a scalar multiplication factor, independent of Peclét number) the anisotropic portion of the average mobility is formally equivalent to the direct diffusive contribution to the particle stress in the context of suspension rheology.

The analysis focuses mainly on the case of simple shear flow. The approximate calculation in the limit of large Peclét numbers, $Pe \gg 1$, which makes extensive use of the 'natural coordinates' along Jeffery orbits previously introduced by Leal & Hinch, verifies that, if the external force is non-orthogonal to the direction along which (undisturbed) fluid velocity variations occur, two of the eigenvalues of $\boldsymbol{D}^C$ are proportional to Pe; moreover, one of these $O(Pe)$ eigenvalues is *negative*. When the external force is parallel to the latter direction, the negative eigenvalue corresponds to the principal direction of contraction in the shear velocity field; this thus relates the non-positive nature of $\boldsymbol{D}^C$ to the interaction between the Taylor dispersion mechanism and the (deterministic) convection within the shear field.

Explicit results for the variation of the dyadics $\bar{\boldsymbol{M}}$, $\boldsymbol{D}^C$ and $\bar{\boldsymbol{D}}^C$ jointly with the respective magnitude of the shear rate and the deviation of the particle geometry from a spherical shape are presented for spheroidal particles. Among other things, it is demonstrated that the proposed definition of the modified Taylor dispersivity coefficient, $\bar{\boldsymbol{D}}^C$, does indeed yield a non-negative dyadic.

1. Introduction: formulation of the problem

Transport in shear flows of Brownian particles lies at the heart of a wide variety of environmental (e.g. the dispersion of pollutants in rivers and the atmosphere), physiological (e.g. the transport of tracers, contaminants, or nutrients in blood flow) and engineering (e.g. mixing) processes. In many instances the distance from the point where the particles are introduced into the flow to the nearest boundary of the suspending fluid domain, as well as the lengthscale over which fluid velocity-gradient variations take place, are 'large' (in some loose sense). This fact allows a simplified formulation of the actual problem, by considering instead transport of the particles in an *unbounded* homogeneous (linear) shear flow.

Existing literature has, by and large, concentrated on the diffusion of *spherical* Brownian particles in homogeneous shear flows (Elrick 1962; Frankel & Acrivos 1968; San Miguel & Sancho 1979; Foister & van de Ven 1980; Dufty 1984; Hess & Rainwater 1984; Leighton 1989, to mention just a few contributions; but see Sarman, Evans & Cummings 1991, for a slight variant of these). The goal of the present contribution is thus to examine the influence of the orientational degrees of freedom on the transport in homogeneous shear flows of *non-spherical* Brownian particles. Specifically, we focus on the contribution to such transport processes of the Taylor dispersion mechanism arising from interaction between the rotary diffusion of such particles and the orientational dependence of their translational velocities.

Assuming the suspension to be dilute, we consider here the motion of a single tracer particle, whose shape we suppose to be axisymmetric (as well as possessing fore–aft symmetry). The geometric configuration of such a rigid body is completely specified by the position $\boldsymbol{R} \equiv (x, y, z)$ in three-dimensional physical space of its centre together with its instantaneous orientation, represented by $\boldsymbol{e}$, a body-fixed unit vector lying along the particle's symmetry axis (see figure 1). The statistical description of the particle's motion is embodied in the conditional probability density $P \equiv P(\boldsymbol{R}, \boldsymbol{e}, t \mid \boldsymbol{R}', \boldsymbol{e}')$, denoting the probability of finding the particle at time $t > 0$ with its centre situated at the physical-space position $\boldsymbol{R}$, and possessing the orientation $\boldsymbol{e}$, given that the particle was originally introduced at time $t = 0$ at position $\boldsymbol{R}'$ with the orientation $\boldsymbol{e}'$. This probability density satisfies the continuity equation

$$\partial P/\partial t + \nabla_R \cdot \boldsymbol{J} + \nabla_e \cdot \boldsymbol{j} = 0, \tag{1.1}$$

in which

$$\boldsymbol{J} = [\boldsymbol{V}(\boldsymbol{R}') + (\boldsymbol{R} - \boldsymbol{R}') \cdot \boldsymbol{G} + \boldsymbol{F} \cdot \boldsymbol{M}(\boldsymbol{e})]\, P - \boldsymbol{D}(\boldsymbol{e}) \cdot \nabla_R P \tag{1.2}$$

and

$$\boldsymbol{j} = \dot{\boldsymbol{e}} P - d_r \nabla_e P \tag{1.3}$$

are, respectively, the physical- and orientational-space flux density vectors. In the latter, $\dot{\boldsymbol{e}} \equiv \mathrm{d}\boldsymbol{e}/\mathrm{d}t$ is the 'convective' (deterministic) time rate of change of the particle's orientation which, for the present case, is given by the expression (cf. Brenner & Condiff 1974)

$$\dot{\boldsymbol{e}} = \boldsymbol{e} \cdot \boldsymbol{\Lambda} + \lambda(\boldsymbol{I} - \boldsymbol{ee})\, \boldsymbol{e} : \boldsymbol{S}, \tag{1.4}$$

in which $\boldsymbol{\Lambda} = \frac{1}{2}(\boldsymbol{G} - \boldsymbol{G}^{\dagger})$ and $\boldsymbol{S} = \frac{1}{2}(\boldsymbol{G} + \boldsymbol{G}^{\dagger})$ are, respectively, the antisymmetric and symmetric portions of the undisturbed, homogeneous fluid-velocity gradient $\boldsymbol{G}$, and $\boldsymbol{I}$ is the dyadic idemfactor. Moreover $\boldsymbol{F}$ is the (constant) external force, typically gravity, acting on the particle, assumed to be independent of the particle's position $\boldsymbol{R}$ and orientation $\boldsymbol{e}$, as well as of the time t. Additionally, in the foregoing, $\boldsymbol{M}(\boldsymbol{e})$ is the translational mobility dyadic, which in body-fixed axes may be written in the transversely isotropic form

$$\boldsymbol{M} = M_{\parallel} \boldsymbol{ee} + M_{\perp}(\boldsymbol{I} - \boldsymbol{ee}) \tag{1.5}$$

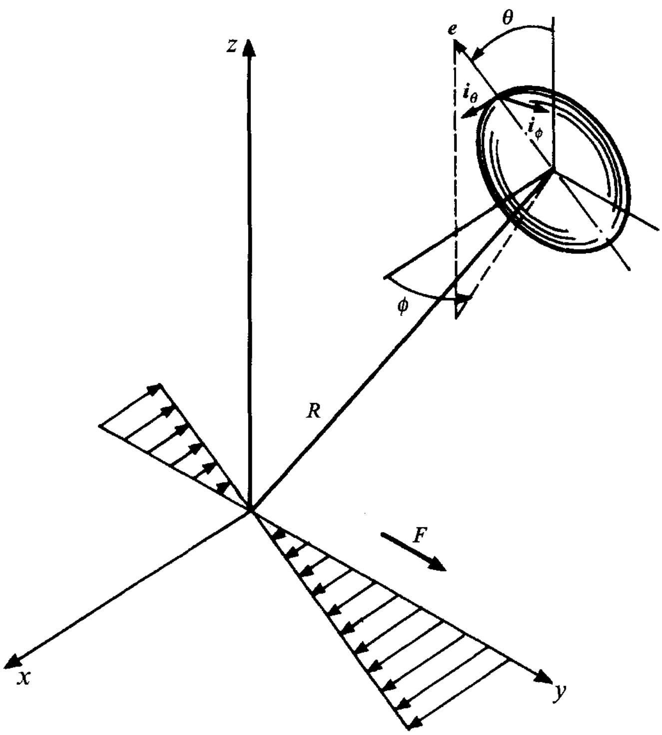

FIGURE 1. Definition of the axisymmetric particle's position $R \equiv (x, y, z)$ and orientation $\boldsymbol{e} \equiv (\theta, \phi)$.

appropriate to a body of revolution; the constant scalars $M_\parallel$ and $M_\perp$ correspond, respectively, to translational motions parallel and perpendicular to the axis of symmetry of the particle. The translational diffusivity dyadic may be obtained from knowledge of the mobility via the Stokes–Einstein relation,

$$\boldsymbol{D} = kT\boldsymbol{M} \tag{1.6}$$

(cf. Brenner 1967), with k Boltzmann's constant and T the absolute temperature. The scalars d_r and λ are, respectively, the rotary diffusion coefficient for particle rotation perpendicular to the symmetry axis and the intrinsic rotational shear-diffusion coefficient. As $V(\boldsymbol{R}')$ represents the undisturbed fluid-velocity vector at the physical space position $\boldsymbol{R}'$, the sum $V + (\boldsymbol{R} - \boldsymbol{R}') \cdot \boldsymbol{G}$ is the undisturbed fluid velocity existing at $\boldsymbol{R}$. Furthermore,

$$\nabla_R \equiv \frac{\partial}{\partial \boldsymbol{R}} \equiv \left(\frac{\partial}{\partial x}, \frac{\partial}{\partial y}, \frac{\partial}{\partial z}\right) \tag{1.7a}$$

and

$$\nabla_e \equiv \frac{\partial}{\partial \boldsymbol{e}} \equiv \boldsymbol{i}_\theta \frac{\partial}{\partial \theta} + \boldsymbol{i}_\phi \frac{1}{\sin\theta} \frac{\partial}{\partial \phi} \tag{1.7b}$$

are, respectively, the physical- and orientation-space gradient operators. (Here ($\boldsymbol{e}$, $\boldsymbol{i}_\theta$, $\boldsymbol{i}_\phi$) is a right-handed triad of body-fixed unit vectors in a frame attached to the particle, with $\boldsymbol{e} \equiv \boldsymbol{e}(\theta, \phi)$ the spherical polar unit radial vector, in which (θ, ϕ) are the spherical polar (Eulerian) angles parameterizing the orientation of the particle relative to a set of space-fixed Cartesian axes, cf. figure 1.)

The continuity and constitutive equations (1.1)–(1.3) are supplemented by the boundary conditions

$$|\boldsymbol{R}-\boldsymbol{R}'|^m\,(P,\boldsymbol{J},\boldsymbol{j}) = (0,\boldsymbol{0},\boldsymbol{0}) \quad \text{as} \quad |\boldsymbol{R}-\boldsymbol{R}'| \to \infty \quad (m = 0,1,2,\dots), \tag{1.8}$$

assuring *inter alia* that P decays exponentially rapidly at large distances from the point $\boldsymbol{R}'$ of initial introduction of the particle into the system. Additionally, it is required that P be continuous and single-valued in the orientation-space variable $\boldsymbol{e}$ (which space can be represented effectively by S_2, the surface of a unit sphere). To the foregoing we adjoin the initial condition

$$P = \begin{cases} \delta(\boldsymbol{R}-\boldsymbol{R}')\,\delta(\boldsymbol{e}-\boldsymbol{e}') & (t=0) \\ 0 & (t<0), \end{cases} \tag{1.9}$$

where the Dirac-delta-function distributions possess the explicit representations

$$\delta(\boldsymbol{R}-\boldsymbol{R}') = \delta(x-x')\,\delta(y-y')\,\delta(z-z') \tag{1.10a}$$

and

$$\delta(\boldsymbol{e}-\boldsymbol{e}') = (\sin\theta)^{-1}\,\delta(\theta-\theta')\,\delta(\phi-\phi'). \tag{1.10b}$$

The initial- and boundary-value problem posed by (1.1)–(1.3), (1.8) and (1.9) uniquely determines $P \geqslant 0$, which is readily shown to satisfy the normalization condition

$$\int_{\boldsymbol{R}_\infty}\int_{S_2} P\,\mathrm{d}^2\boldsymbol{e}\,\mathrm{d}^3\boldsymbol{R} = 1 \quad \text{for all} \quad t \geqslant 0, \tag{1.11}$$

requiring that the total probability of finding the (centre of the) tracer particle somewhere within the phase space be conserved. In the latter relation, $\mathrm{d}^3\boldsymbol{R} \equiv \mathrm{d}x\,\mathrm{d}y\,\mathrm{d}z$ is a physical-space volume element and $\mathrm{d}^2\boldsymbol{e} \equiv (\sin\theta)\,\mathrm{d}\theta\,\mathrm{d}\phi$ is an areal element on the surface of the unit sphere. Furthermore, the solution of the foregoing 'instantaneous source' problem can serve as the appropriate Green's function for the more general problem where (1.9) is replaced by an arbitrary initial distribution.

The calculation of P is a rather formidable task requiring the solution of the above initial- and boundary-value problem within the five-dimensional phase space $\boldsymbol{R}_\infty \oplus S_2$. (In fact, the only previous attempt to address this problem of which we are aware was made by Cerda & van de Ven (1983), who examined the translational motion of a neutrally buoyant Brownian spheroid in simple shear flow. Assuming large rotary Peclét numbers (cf. (2.22)), they *decoupled* the translational and rotary motions (in a manner which does not appear to us to be entirely consistent).) However, one is generally not interested in the exhaustively detailed information provided by knowledge of the exact solution P, but rather only in its orientational average,

$$\bar{P}(\boldsymbol{R},t\,|\,\boldsymbol{R}',\boldsymbol{e}') \overset{\text{def}}{=} \int_{S_2} P\,\mathrm{d}^2\boldsymbol{e}, \tag{1.12}$$

describing transport of the particle (centre) within physical space, irrespective of the particle's instantaneous orientation.

In the next section we make use of a recent extension (Frankel & Brenner 1991) of generalized Taylor dispersion theory, enabling us to obtain a long-time asymptotic description of $\bar{P}$ that does not require *a priori* knowledge of P itself. This latter, coarse-grained, approximation consists of the formulation in physical space of a model convection–diffusion problem characterized by a pair of constant phenomenological coefficients respectively representing the particle's mean velocity and dispersivity. Subsequent sections present the calculation of these coefficients in the asymptotic cases of small and large rotary Peclét numbers (§3 and §4, respectively) and for arbitrary Peclét numbers (in §5). Explicit results are obtained in §6 for spheroidal particles, which provide the basis for a discussion of the respective effects of the magnitude of shear rate and of the geometry of the particles (i.e. its deviation from a spherical shape) upon the mean transport process in physical space.

2. Recapitulation of generalized Taylor dispersion theory for homogeneous shear flows

The problem formulation outlined in the preceding section is readily verified to conform to that of the generic problem underlying generalized Taylor dispersion theory when one recognizes the equivalence relations

$$\boldsymbol{R} \rightarrow \boldsymbol{Q}, \quad \boldsymbol{e} \rightarrow \boldsymbol{q}, \tag{2.1 a, b}$$

which identify the physical-space position and orientation of the particle with the respective 'global' and 'local' coordinates of the abstract multidimensional phase space $\boldsymbol{Q}_\infty \oplus \boldsymbol{q}_0$ of the latter theory. Upon making use of the results of Frankel & Brenner (1991) for unbounded, homogeneous shear fields, it is established that when the eigenvalues ν_i of $\boldsymbol{G}$ are purely imaginary,† i.e.

$$\mathrm{Re}\{\nu_i\} = 0 \quad (i = 1,2,3), \tag{2.2}$$

(with Re{} denoting the real part of the quantity in braces), the leading-order long-time $(d_r t \gg 1)$ asymptotic behaviour of $\bar{P}$ is given by the solution of the 'model' convection–diffusion problem,

$$\partial \bar{P}/\partial t + \nabla_{\boldsymbol{R}} \cdot \bar{\boldsymbol{J}} = 0, \tag{2.3a}$$

$$\bar{\boldsymbol{J}} = [V(\boldsymbol{R}') + (\boldsymbol{R}-\boldsymbol{R}) \cdot \boldsymbol{G} + \bar{\boldsymbol{U}}]\bar{P} - \bar{\boldsymbol{D}} \cdot \nabla_{\boldsymbol{R}} \bar{P}, \tag{2.3b}$$

subject to the boundary conditions

$$|\boldsymbol{R}-\boldsymbol{R}'|^m(\bar{P},\bar{\boldsymbol{J}}) \rightarrow (0,\boldsymbol{0}) \quad \text{as} \quad |\boldsymbol{R}-\boldsymbol{R}'| \rightarrow \infty \quad (m = 0,1,2,\dots), \tag{2.4a}$$

and initial condition

$$\bar{P} = \begin{cases} \delta(\boldsymbol{R}-\boldsymbol{R}') & (t=0) \\ 0 & (t<0). \end{cases} \tag{2.4b}$$

These equations constitute the purely physical-space counterpart of the exact equations (1.1), (1.2), (1.8) and (1.9), respectively.

The constant (i.e. time-, position- and orientation-independent) phenomenological coefficients $\bar{\boldsymbol{U}}$ and $\bar{\boldsymbol{D}}$ appearing in the model flux-vector constitutive equation (2.3*b*) are related to the long-time asymptotic rates of change (for $m = 1$ and 2) of the total statistical polyadic moments

$$\boldsymbol{M}_m \stackrel{\text{def}}{=} \int_{\boldsymbol{R}_\infty} \int_{S_2} (\boldsymbol{R}-\boldsymbol{R}')^m P \,\mathrm{d}^2\boldsymbol{e}\, \mathrm{d}^3\boldsymbol{R} \quad (m = 0,1,2,\dots)$$

† As explained in the general theory (Frankel & Brenner 1991), the kinematical significance of this restriction is that it excludes the possibility that $\boldsymbol{R}$, the position of the particle in physical space, diverges exponentially rapidly as a result of passive convection in the shear field. Thus (2.2) renders the latter a 'slow' process relative to the (exponentially rapid) relaxation of the orientational distribution via rotary Brownian diffusion.

of the probability density. The existence of these moments is guaranteed by the boundary condition (1.8), which assures that the preceding momental integrals converge. The 'classical' paradigmatic definitions (cf. Brenner 1980, 1982), namely

$$\bar{U} = \lim_{t\to\infty} \frac{\mathrm{d}\boldsymbol{M}_1}{\mathrm{d}t} \tag{2.5a}$$

and

$$\bar{\boldsymbol{D}} = \lim_{t\to\infty} \frac{1}{2}\frac{\mathrm{d}}{\mathrm{d}t}(\boldsymbol{M}_2 - \boldsymbol{M}_1\boldsymbol{M}_1), \tag{2.5b}$$

of the macroscale phenomenological coefficients $\bar{U}$ and $\bar{\boldsymbol{D}}$, fail in the present problem to yield stationary and invariant coefficients because, when $\boldsymbol{G} \neq \boldsymbol{0}$, the asymptotic behaviour of $\boldsymbol{M}_1$ and $\boldsymbol{M}_2 - \boldsymbol{M}_1\boldsymbol{M}_1$ is nonlinear in t. It is, however, observed in Frankel & Brenner (1991) that, for long times, the respective codeformational ('Oldroyd') rates of change do attain stationary and invariant limits, namely

$$\lim_{t\to\infty} \frac{\delta \boldsymbol{M}_1}{\delta t} \stackrel{\text{def}}{=} \lim_{t\to\infty}\left(\frac{\mathrm{d}\boldsymbol{M}_1}{\mathrm{d}t} - \boldsymbol{M}_1\cdot\boldsymbol{G}\right) \equiv V(\boldsymbol{R}') + U^* \tag{2.6}$$

and

$$\lim_{t\to\infty}\frac{1}{2}\frac{\delta}{\delta t}(\boldsymbol{M}_2 - \boldsymbol{M}_1\boldsymbol{M}_1)$$

$$\stackrel{\text{def}}{=} \lim_{t\to\infty}\frac{1}{2}\left[\frac{\mathrm{d}}{\mathrm{d}t}(\boldsymbol{M}_2 - \boldsymbol{M}_1\boldsymbol{M}_1) - (\boldsymbol{M}_2 - \boldsymbol{M}_1\boldsymbol{M}_1)\cdot\boldsymbol{G} - \boldsymbol{G}^\dagger\cdot(\boldsymbol{M}_2 - \boldsymbol{M}_1\boldsymbol{M}_1)\right] \equiv \boldsymbol{D}^*. \tag{2.7}$$

The foregoing codeformational derivatives (cf. Bird, Armstrong & Hassager 1987) eliminate the contribution of the rate of passive convection of the tracer particle in the shear field. Thus, U^* represents the average 'slip velocity' of the particle relative to the fluid, while $\boldsymbol{D}^*$ represents the rate of spread of a 'cloud' of solute particles without the contribution of the shear to the rate of distortion of this cloud.

The constants U^* and $\boldsymbol{D}^*$ are respectively obtained via the following quadratures over the orientational space:

$$U^* = \bar{\boldsymbol{M}}\cdot F, \tag{2.8a}$$

where

$$\bar{\boldsymbol{M}} \stackrel{\text{def}}{=} \int_{S_2} P_0^\infty(\boldsymbol{e})\,\boldsymbol{M}(\boldsymbol{e})\,\mathrm{d}^2\boldsymbol{e} \tag{2.8b}$$

is the mean translational mobility dyadic, and

$$\boldsymbol{D}^* = \boldsymbol{D}^M + \boldsymbol{D}^C, \tag{2.9a}$$

in which

$$\boldsymbol{D}^M \stackrel{\text{def}}{=} \int_{S_2} P_0^\infty(\boldsymbol{e})\,\boldsymbol{D}(\boldsymbol{e})\,\mathrm{d}^2\boldsymbol{e} \equiv kT\bar{\boldsymbol{M}} \tag{2.9b}$$

(cf. (1.6)), and

$$\boldsymbol{D}^C \stackrel{\text{def}}{=} \int_{S_2} P_0^\infty(\boldsymbol{e})\,[\![B(\boldsymbol{e})\,\boldsymbol{M}(\boldsymbol{e})\cdot F]\!]^s\,\mathrm{d}^2\boldsymbol{e} \tag{2.9c}$$

are, respectively, the 'molecular' and 'Taylor' contributions to the dispersivity dyadic $\boldsymbol{D}^*$. In the latter relation, the operator $[\![\;]\!]^s$ denotes the fully symmetrized polyadic appearing within the double brackets; the orientation-specific fields P_0^∞ and $\boldsymbol{B}$ are to be defined presently.

Equations (2.6) and (2.7) represent the natural extension to shear flows of the classical (Brenner 1980, 1982) Taylor dispersion expressions (2.5*a*) and (2.5*b*), respectively; indeed, choosing

$$\bar{\boldsymbol{U}} = \boldsymbol{U}^*, \quad \bar{\boldsymbol{D}} = \boldsymbol{D}^* \tag{2.10a, b}$$

assures the long-time matching of the leading-order temporal asymptotic behaviour of the statistical moments of the respective solutions of the exact and model problems. However, by making use of the equations governing the vector $\boldsymbol{B}$-field (see (2.19) below) in conjunction with some vector identities, one can show that

$$\boldsymbol{D}^* = \bar{\boldsymbol{D}}^* - \left[\!\!\left[\int_{S_2} P_0^\infty \boldsymbol{B}\boldsymbol{B} \,\mathrm{d}^2\boldsymbol{e} \cdot \boldsymbol{G} \right]\!\!\right]^s, \tag{2.11a}$$

where

$$\bar{\boldsymbol{D}}^* = \int_{S_2} P_0^\infty [\boldsymbol{D} + d_r (\nabla_e \boldsymbol{B})^\dagger \cdot \nabla_e \boldsymbol{B}] \,\mathrm{d}^2\boldsymbol{e}, \tag{2.11b}$$

which latter dyadic is clearly positive-definite. While $\boldsymbol{D}^* = \bar{\boldsymbol{D}}^*$ when $\boldsymbol{G} = \boldsymbol{0}$, the former may not be non-negative when $\boldsymbol{G} \neq \boldsymbol{0}$. Frankel & Brenner (1991) have established that within the framework of the leading-order approximation, long-time matching is still achieved when (2.10*b*) is replaced by

$$\bar{\boldsymbol{D}} = \bar{\boldsymbol{D}}^*. \tag{2.12}$$

This choice also ensures that the solution of the model problem is well behaved at all times.

The scalar field $P_0^\infty(\boldsymbol{e})$, defined by the long-time limit of the zero-order, 'local' moment field (Brenner 1980),

$$P_0(\boldsymbol{e}, t \,|\, \boldsymbol{R}', \boldsymbol{e}') = \int_{R_\infty} P(\boldsymbol{R}, \boldsymbol{e}, t \,|\, \boldsymbol{R}', \boldsymbol{e}') \,\mathrm{d}^3\boldsymbol{R}, \tag{2.13}$$

represents the conditional probability density of finding the particle possessing the orientation $\boldsymbol{e}$, irrespective of its instantaneous physical space position $\boldsymbol{R}$, given its initial position $\boldsymbol{R}'$ and orientation $\boldsymbol{e}'$. The fact that the long-time limit of P_0 is a stationary and invariant (i.e. independent of both t and $\boldsymbol{e}'$) equilibrium orientation distribution constitutes a fundamental feature of the generalized Taylor dispersion paradigm. In the present problem, $P_0^\infty(\boldsymbol{e})$ satisfies the rotational convective–diffusion equation (cf. Frankel & Brenner 1991, their equation (3.6))

$$\nabla_e \cdot (\dot{\boldsymbol{e}} P_0^\infty - d_r \nabla_e P_0^\infty) = 0, \tag{2.14a}$$

along with the normalization condition

$$\int_{S_2} P_0^\infty \,\mathrm{d}^2\boldsymbol{e} = 1 \tag{2.14b}$$

and the requirement of continuity and single-valuedness on S_2. The above problem is identical to that posed for the steady-state orientational distribution function in a homogeneous shear flow of a dilute suspension whose particles are uniformly distributed throughout physical space. This latter problem has been extensively studied in the contexts of streaming birefringence and rheology of suspensions (Burgers 1938; Peterlin 1938; Scheraga, Edsall & Gadd 1951; Scheraga 1955; Leal & Hinch 1971; Hinch & Leal 1972; Stewart & Sorensen 1972; Brenner & Condiff 1974; Krushkal & Gallily 1984, to cite just a few contributions).

Use is made of the foregoing equivalence in subsequent sections. Here, we point out another useful equivalence, which is a corollary of the former one. To this end we define

$$\Delta\bar{\boldsymbol{M}} \overset{\text{def}}{=} \bar{\boldsymbol{M}} - \tfrac{1}{3}(M_{\parallel} + 2M_{\perp})\boldsymbol{I}. \tag{2.15}$$

As such, $\Delta\bar{\boldsymbol{M}}$ expresses the departure of the average translational mobility $\bar{\boldsymbol{M}}$ from the isotropic result corresponding to sedimentation in a quiescent fluid (Brenner & Condiff 1972). Substitute (1.5) and (2.15) into the definition (2.8 *b*) to obtain

$$\Delta\bar{\boldsymbol{M}} = (M_{\parallel} - M_{\perp})\left(\int_{S_2} P_0^{\infty}(\boldsymbol{e})\,\boldsymbol{ee}\,\mathrm{d}^2\boldsymbol{e} - \tfrac{1}{3}\boldsymbol{I}\right). \tag{2.16}$$

Thus, $\Delta\bar{\boldsymbol{M}}$ involves the same orientational moments ('goniometric factors') as those appearing in $\boldsymbol{\tau}^D$, the 'direct' rotary diffusion contribution to the particle stress in the context of suspension rheology (cf. Brenner 1972).

The vector $\boldsymbol{B}(\boldsymbol{e})$-field is defined by the long-time limit

$$\boldsymbol{B}(\boldsymbol{e}) = \lim_{t\to\infty}\left(\frac{\boldsymbol{P}_1}{P_0} - \boldsymbol{M}_1\right), \tag{2.17}$$

where
$$\boldsymbol{P}_1(\boldsymbol{e}, t\,|\,\boldsymbol{R}', \boldsymbol{e}') = \int_{R_\infty} \boldsymbol{R}P(\boldsymbol{R}, \boldsymbol{e}, t\,|\,\boldsymbol{R}', \boldsymbol{e}')\,\mathrm{d}^3\boldsymbol{R} \tag{2.18}$$

is, by definition, the first-order, local moment of the distribution function P. As such, the first term appearing on the right-hand side of (2.17) represents the average physical-space position of the tracer given that its instantaneous orientation is $\boldsymbol{e}$, whereas $\boldsymbol{M}_1$ represents the average position without the latter constraint. That the long-time limit of the difference between these two average positions is indeed the stationary and invariant vector $\boldsymbol{B}(\boldsymbol{e})$-field is established by Frankel & Brenner (1991, §5). In the present context, $\boldsymbol{B}$ is governed by the boundary-value problem

$$\nabla_e \cdot [\dot{\boldsymbol{e}}P_0^{\infty}\boldsymbol{B} - d_r \nabla_e(P_0^{\infty}\boldsymbol{B})] - P_0^{\infty}\boldsymbol{B}\cdot\boldsymbol{G} = P_0^{\infty}(\boldsymbol{M} - \bar{\boldsymbol{M}})\cdot\boldsymbol{F} \tag{2.19a}$$

in conjunction with the normalization condition

$$\int_{S_2} P_0^{\infty}\boldsymbol{B}\,\mathrm{d}^2\boldsymbol{e} = \boldsymbol{0}, \tag{2.19b}$$

together with the requirements of continuity and single-valuedness on S_2.

For future reference it is useful to express the problems formulated above for P_0^{∞} and $\boldsymbol{B}$ explicitly in terms of the Eulerian angles (θ, ϕ) relative to a space-fixed Cartesian system. Towards this end, write

$$\dot{\boldsymbol{e}} = G\hat{\dot{\boldsymbol{e}}}, \tag{2.20a}$$

where G is some appropriate norm of $\boldsymbol{G}$ (cf. (2.26)) and

$$\hat{\dot{\boldsymbol{e}}} = \boldsymbol{i}_\theta\dot{\theta} + \boldsymbol{i}_\phi\dot{\phi}\sin\theta, \tag{2.20b}$$

in which $\dot{\theta}(\theta, \phi)$ and $\dot{\phi}(\theta, \phi)$ are dimensionless rates of change (obtainable from (1.4) once $\boldsymbol{G}$ is specified). Substitute (2.20) into (2.14) and utilize the definition (1.7 *b*) of ∇_e to obtain

$$Pe\left[\frac{1}{\sin\theta}\frac{\partial}{\partial\theta}(P_0^{\infty}\dot{\theta}\sin\theta) + \frac{\partial}{\partial\phi}(P_0^{\infty}\dot{\phi})\right] - \left[\frac{1}{\sin\theta}\frac{\partial}{\partial\theta}\left(\frac{\partial P_0^{\infty}}{\partial\theta}\sin\theta\right) + \frac{1}{\sin^2\theta}\frac{\partial^2 P_0^{\infty}}{\partial\phi^2}\right] = 0 \tag{2.21a}$$

and
$$\int_0^{\pi}\int_0^{2\pi} P_0^{\infty} \sin\theta \, d\phi \, d\theta = 1, \tag{2.21b}$$
with
$$Pe = G/d_r \tag{2.22}$$
the rotary Peclét number. Define the dimensionless dyadic field $\boldsymbol{b}(\boldsymbol{e})$ via the expression

$$P_0^{\infty} \boldsymbol{B} \stackrel{\text{def}}{=} \frac{(M_{\parallel} - M_{\perp}) F}{d_r} \boldsymbol{b} \cdot \hat{\boldsymbol{F}}, \tag{2.23}$$

where $F = |\boldsymbol{F}|$ and $\hat{\boldsymbol{F}} = \boldsymbol{F}/F$, and use (1.5), (2.8), (2.20) and (2.22), to obtain from (2.19) the following equations governing the scalar components of $\boldsymbol{b} = b_{ij}(\theta, \phi)$ $(i,j = 1,2,3)$:

$$Pe\left[\frac{1}{\sin\theta}\frac{\partial}{\partial\theta}(b_{ij}\,\dot{\theta}\sin\theta) + \frac{\partial}{\partial\phi}(b_{ij}\,\dot{\phi})\right] - \left[\frac{1}{\sin\theta}\frac{\partial}{\partial\theta}\left(\frac{\partial}{\partial\theta}(b_{ij})\sin\theta\right) + \frac{1}{\sin^2\theta}\frac{\partial^2}{\partial\phi^2}(b_{ij})\right]$$
$$- Pe\, \hat{G}_{ik}^{\dagger} b_{kj} = P_0^{\infty}(f_{ij} - \bar{f}_{ij}), \tag{2.24a}$$

together with
$$\int_0^{\pi}\int_0^{2\pi} b_{ij} \sin\theta \, d\phi \, d\theta = 0. \tag{2.24b}$$

In the last term on the left-hand side of (2.24*b*), $\hat{\boldsymbol{G}} = \boldsymbol{G}/G$ is the dimensionless velocity gradient; moreover, summation on repeated indices is implied. In the forcing term appearing on the right-hand side of (2.24*a*), f_{ij} denotes the Cartesian components of the dyad $\boldsymbol{ee}$ in the space-fixed frame, whereas

$$\bar{f}_{ij} \stackrel{\text{def}}{=} \int_0^{\pi}\int_0^{2\pi} P_0^{\infty}(\boldsymbol{ee})_{ij} \sin\theta \, d\phi \, d\theta. \tag{2.25}$$

Much of the subsequent development focuses on the case of simple shear flow, where the fluid velocity is taken to be (cf. figure 1)

$$\boldsymbol{V} = \boldsymbol{i}_1 G y. \tag{2.26}$$

(For this flow, the eigenvalues of $\boldsymbol{G}$ are $\nu_i = 0$ $(i = 1,2,3)$; thus, the requirement (2.2) of the general theory is trivially satisfied.) From (1.4) and (2.20) we find for this shear flow that

$$\dot{\theta} = \tfrac{1}{4}\lambda \sin 2\theta \sin 2\phi, \quad \dot{\phi} = \tfrac{1}{2}(\lambda \cos 2\phi - 1). \tag{2.27a, b}$$

Additionally, the general coupling which exists between the (2.24*a*) for the various b_{ij} is somewhat relaxed, since these can now be written as

$$Pe\left[\frac{1}{\sin\theta}\frac{\partial}{\partial\theta}(b_{ij}\,\dot{\theta}\sin\theta) + \frac{\partial}{\partial\phi}(b_{ij}\,\dot{\phi})\right] - \left[\frac{1}{\sin\theta}\frac{\partial}{\partial\theta}\left(\frac{\partial}{\partial\theta}(b_{ij})\sin\theta\right) + \frac{1}{\sin^2\theta}\frac{\partial^2}{\partial\phi^2}(b_{ij})\right]$$
$$= P_0^{\infty}(f_{ij} - \bar{f}_{ij}) + Pe\,\delta_{i1} b_{2j}, \tag{2.28}$$

where δ_{ij} is the Kronecker delta.

In the following sections we address the calculation of P_0^{∞} and $\boldsymbol{b}$. This accomplished, one can proceed to evaluate the resulting macroscopic phenomenological coefficients.

3. Dispersion in weak (homogeneous) shear ($Pe \ll 1$)

The case where Brownian rotation dominates the effect of the shear on the orientational distribution function (corresponding to small Peclét numbers, $Pe \ll 1$) is analysed in this section. In particular, upon making use of polyadic surface spherical harmonics (Brenner 1964*a*, *b*), the respective asymptotic expansions for the scalar field

$P_0^\infty(\boldsymbol{e})$ and vector field $P_0^\infty \boldsymbol{B}(\boldsymbol{e})$ are both obtained in invariant form (for arbitrary homogeneous weak shear field), from which the macroscopic transport coefficients for a homogeneous axisymmetric and centrosymmetric particle are subsequently calculated.

3.1. *Calculation of* P_0^∞

As observed above, the problem posed for P_0^∞, namely (2.14) in conjunction with (1.4), is formally equivalent to that for the steady-state orientational distribution function arising from the homogeneous shear of a suspension of non-spherical Brownian particles when these are uniformly distributed throughout physical space. We thus simply adopt the solution of the latter problem, already available in the literature (cf. Brenner & Condiff 1974), namely

$$P_0^\infty \approx \frac{1}{4\pi}\{1+\tfrac{1}{2}\lambda Pe\, \boldsymbol{ee}:\hat{\boldsymbol{S}}+Pe^2\,[\tfrac{1}{8}\lambda^2 \boldsymbol{eeee}(\,\cdot\,)^4\,\hat{\boldsymbol{S}}\hat{\boldsymbol{S}}-\tfrac{1}{60}\lambda^2\hat{\boldsymbol{S}}:\hat{\boldsymbol{S}}$$

$$-\tfrac{1}{60}\lambda \boldsymbol{ee}:(\hat{\boldsymbol{\Lambda}}\cdot\hat{\boldsymbol{S}})]+O(Pe^3)\}, \quad (3.1)$$

where $\hat{\boldsymbol{S}}$ and $\hat{\boldsymbol{\Lambda}}$ are, respectively, the symmetric and antisymmetric parts of the dimensionless velocity gradient $\hat{\boldsymbol{G}}$, and $(\,\cdot\,)^m$ denotes m successive scalar contractions.

3.2. *Average translational mobility*

Substitute (3.1) into (2.16) to obtain the dimensionless form of $\Delta\bar{\boldsymbol{M}}$, (2.15), namely

$$\delta^M \overset{\text{def}}{=} \frac{\Delta\bar{\boldsymbol{M}}}{\tfrac{1}{3}(M_\parallel+2M_\perp)} = \frac{1}{5}\frac{M_\parallel-M_\perp}{M_\parallel+2M_\perp}\Delta\hat{\bar{\boldsymbol{M}}}, \quad (3.2a)$$

wherein (cf. Brenner & Condiff 1974)

$$\Delta\hat{\bar{\boldsymbol{M}}} \approx \lambda Pe\,\hat{\boldsymbol{S}}+\tfrac{1}{21}\lambda^2 Pe^2[3\hat{\boldsymbol{S}}\cdot\hat{\boldsymbol{S}}-(\hat{\boldsymbol{S}}:\hat{\boldsymbol{S}})\boldsymbol{I}\}-\tfrac{1}{6}\lambda Pe^2(\hat{\boldsymbol{\Lambda}}\cdot\hat{\boldsymbol{S}}-\hat{\boldsymbol{S}}\cdot\hat{\boldsymbol{\Lambda}})+\mathrm{O(Pe^3)} \quad (3.2b)$$

exclusively represents the functional dependence of $\Delta\bar{\boldsymbol{M}}$ upon Pe. (The scalar factor multiplying $\Delta\hat{\bar{\boldsymbol{M}}}$ in (3.2a) depends solely upon the shape of the particle.)

3.3. *The dyadic* $\boldsymbol{b}$ *field*

Upon substituting the definitions (2.20a) and (2.23) into (2.19) one obtains the differential equation

$$\nabla_e^2 \boldsymbol{b}-Pe\,\nabla_e\cdot(\dot{\boldsymbol{e}}\boldsymbol{b})+Pe\,\hat{\boldsymbol{G}}^\dagger\cdot\boldsymbol{b} = -P_0^\infty\frac{\boldsymbol{M}-\bar{\boldsymbol{M}}}{M_\parallel-M_\perp} \quad (3.3a)$$

in conjunction with the normalization condition

$$\int_{S_2}\boldsymbol{b}\,\mathrm{d}^2e = \boldsymbol{0}. \quad (3.3b)$$

Assuming an asymptotic expansion of the form

$$\boldsymbol{b} \approx \boldsymbol{b}_0(\boldsymbol{e})+Pe\,\boldsymbol{b}_1(\boldsymbol{e})+Pe^2\,\boldsymbol{b}_2(\boldsymbol{e})+O(Pe^3) \quad (3.4)$$

and making use of (3.1), (3.2) and (1.5) one arrives at a sequence of boundary-value problems for $\boldsymbol{b}_i$ ($i = 0, 1, 2, \dots$). These are solved recursively† by expressing the forcing terms appearing at each stage in terms of polyadic surface harmonics. The resulting equations are then readily inverted when use is made of the equation (Brenner 1964a, b)

$$\nabla_e^2 P_n = -n(n+1)\,P_n \quad (n = 0, 1, 2, \dots) \quad (3.5)$$

† Details of the calculations outlined here as well as in subsequent sections may be obtained upon request directly from the authors or from the *Journal of Fluid Mechanics* Editorial Office.

satisfied by the polyadic surface spherical harmonic $\boldsymbol{P}_n(\boldsymbol{e})$ of degree n, together with the orthogonality property

$$\int_{S_2} \boldsymbol{P}_m \boldsymbol{P}_n \,\mathrm{d}^2\boldsymbol{e} = \boldsymbol{0} \quad (m \neq n). \tag{3.6}$$

3.4. *Taylor dispersivity*

From (2.9*c*) in conjunction with (1.5), (2.23), (3.3*b*) and the definition

$$\boldsymbol{P}_2 = \tfrac{1}{2}(3\boldsymbol{ee}-\boldsymbol{I}), \tag{3.7}$$

one may write

$$\boldsymbol{D}^C = \frac{(M_{\parallel}-M_{\perp})^2 F^2}{d_r}\hat{\boldsymbol{D}}^C, \tag{3.8a}$$

wherein the dimensionless dyadic

$$\hat{\boldsymbol{D}}^C = \frac{2}{3}\left[\!\!\left[\hat{\boldsymbol{F}}\cdot\int_{S_2} \boldsymbol{P}_2 \boldsymbol{b}\,\mathrm{d}^2\boldsymbol{e}\cdot\hat{\boldsymbol{F}}\right]\!\!\right]^s \tag{3.8b}$$

exclusively represents the functional dependence of $\boldsymbol{D}^C$ upon Pe. A straightforward calculation leads to the small-Peclét-number expansion

$$\hat{\boldsymbol{D}}^C \approx \hat{\boldsymbol{D}}^C_0 + Pe\,\hat{\boldsymbol{D}}^C_1 + Pe^2\,\hat{\boldsymbol{D}}^C_2 + O(Pe^3), \tag{3.9}$$

whose dyadic coefficients are tabulated elsewhere.†

3.5. *Transport coefficients in simple shear*

The invariant results mentioned above are now specialized to the case for which

$$\hat{\boldsymbol{G}} = \begin{pmatrix} 0 & 0 & 0 \\ 1 & 0 & 0 \\ 0 & 0 & 0 \end{pmatrix}, \tag{3.10}$$

corresponding to (2.26).

Average translational mobility

For simple shear, the dimensionless dyadic $\Delta\hat{\boldsymbol{M}}$ (3.2*b*), possesses the eigenvalues

$$\nu_{1,2} \approx \pm\tfrac{1}{2}\lambda Pe + \tfrac{1}{84}\lambda^2 Pe^2 + O(Pe^3), \quad \nu_3 \approx -\tfrac{1}{42}\lambda^2 Pe^2 + O(Pe^3), \tag{3.11a–c}$$

together with the corresponding eigenvectors

$$\boldsymbol{u}_{1,2} \approx (1, \pm 1 - \tfrac{1}{6}Pe, 0), \quad \boldsymbol{u}_3 = (0, 0, 1). \tag{3.12a–c}$$

As could have been anticipated (cf. Brenner & Condiff 1974), the principal directions of $\Delta\hat{\boldsymbol{M}}$ (as well as those of $\bar{\boldsymbol{M}}$) coincide, to the leading order in Peclét number, with those of the strain rate $\hat{\boldsymbol{S}}$. Within this same order of approximation, the eigenvalues ν_1 and ν_2 show, respectively, an increase in the average 'slip velocity' (of the particle relative to the fluid) in the direction $\boldsymbol{u}_1$ of extension, and a comparable decrease in the direction $\boldsymbol{u}_2$ of contraction. With increasing Peclét number the principal directions of $\Delta\bar{\boldsymbol{M}}$ (and $\bar{\boldsymbol{M}}$) rotate about the direction $-\boldsymbol{i}_3$ of the undisturbed vorticity vector, so that $\boldsymbol{u}_1$ becomes closer to the direction $\boldsymbol{i}_1$ of the undisturbed fluid velocity vector. The second-order, $O(Pe^2)$, contributions to ν_i show a uniform increase in the plane $(\boldsymbol{i}_1, \boldsymbol{i}_2)$ of the flow, and a concomitant decrease in the direction of $\boldsymbol{i}_3$. Obviously, the basic conclusions of the foregoing discussion are also attributable to the 'molecular' contribution $\boldsymbol{D}^M$ of the translational diffusivity $\boldsymbol{D}$ to $\boldsymbol{D}^*$ (2.9*a*, *b*).

† Cf. the footnote following (3.4).

Finally, it is worthwhile mentioning that the components of $\Delta\bar{\boldsymbol{M}}$ (not presented explicitly) are essentially the same (up to a normalization factor independent of Pe) as the results of Giesekus (1962) for $\boldsymbol{\tau}^D$, the direct diffusive contribution to the particle stress. This is not surprising in the light of the general equivalence established in the preceding section (cf. (2.16) *et seq.*).

Taylor dispersivity dyadic

In the next section, which deals with the opposite limit of large Peclét numbers, it is concluded that the most significant interaction between 'Taylor' dispersion mechanism and the shear field takes place when $\hat{\boldsymbol{F}} = \boldsymbol{i}_2$, i.e. when the external force acts parallel to the gradient of the undisturbed fluid speed. For subsequent comparison, we focus here too on this case. A straightforward calculation yields the eigenvalues

$$\nu_1 \approx \frac{2}{135} + \frac{Pe^2}{2381400}(174\lambda^2 + 630\lambda + 245), \tag{3.13a}$$

$$\nu_2 \approx \frac{1}{90} - \frac{Pe^2}{11907000}(3159\lambda^2 + 4200\lambda + 1225), \tag{3.13b}$$

$$\nu_3 \approx \frac{1}{90} - \frac{Pe^2}{453600}(11\lambda^2 + 90\lambda + 35), \tag{3.13c}$$

together with the corresponding eigenvectors

$$\boldsymbol{u}_1 \approx \left(\frac{9\lambda+14}{42}Pe, 1, 0\right), \quad \boldsymbol{u}_2 = \left(1, -\frac{9\lambda+14}{42}Pe, 0\right), \quad \boldsymbol{u}_3 = (0,0,1). \tag{3.14a–c}$$

The leading-order values correspond to sedimentation in a quiescent fluid (cf. Brenner 1979). The principal directions $\boldsymbol{u}_2$ and $\boldsymbol{u}_1$, respectively corresponding to the smallest and largest of the above eigenvalues, are rotated with increasing Pe (within the plane of the flow) towards the principal directions of strain, respectively corresponding to pure contraction and pure elongation.

4. Dispersion in simple shear flow: weak-Brownian-rotation limit ($Pe \gg 1$)

This section addresses the dispersion of axisymmetric centrosymmetric Brownian particles in the limit $Pe \gg 1$, where the effect of shear dominates that of rotary Brownian diffusion.† The analysis follows the approach of Leal & Hinch (1971) and makes extensive use of their elegant 'natural' or 'orbit' coordinates (C, τ). These are related to the Eulerian angles through Jeffery's (1922) solution,

$$\theta = \tan^{-1}[C(r^2\sin^2\tau + \cos^2\tau)^{\frac{1}{2}}], \quad \phi = \cot^{-1}(r\tan\tau), \tag{4.1a, b}$$

where

$$\tau = rGt/(r^2+1). \tag{4.1c}$$

4.1. *The field* P_0^∞

In accordance with the comments following (2.14), the problem posed for P_0^∞, (2.21) and (2.27), is formally equivalent to the problem of the steady-state orientational distribution, calculated by Leal & Hinch (1971) and Hinch & Leal (1972). In order to

† In fact, the resulting asymptotic expansions are uniformly valid provided that $Pe \gg r^3 + r^{-3}$, where r is the (equivalent) particle axis ratio. This stronger requirement ensures that the effects of Brownian rotations are weak throughout the entire orientation space, thus excluding the so-called 'intermediate' singular case (Hinch & Leal 1972). This restriction limits somewhat the practical utility of subsequent results by excluding both 'rod-like' ($r \gg 1$) and 'disk-like' ($r \ll 1$) particles.

render unique the limit of weak rotary diffusion, they derive the following integral condition (similar to the result of Batchelor 1956 for closed-streamline flows at large Reynolds numbers):

$$\int_c \mathrm{d}s\, \boldsymbol{\nu}\cdot\boldsymbol{\nabla}_e P_0^\infty = 0, \tag{4.2}$$

where ds is an element of arclength along the closed Jeffery orbit c, and $\boldsymbol{\nu}$ is an outwardly directed unit normal to the contour c, tangent to the surface of the unit sphere. The asymptotic, large-Peclét-number calculation yields for P_0^∞ the expansion

$$P_0^\infty \approx P_0^{\infty(0)}(\boldsymbol{e}) + Pe^{-1} P_0^{\infty(1)}(\boldsymbol{e}) + O(Pe^{-2}), \tag{4.3}$$

whose coefficient functions were obtained by Hinch & Leal (1972).

4.2. *Average translational mobility*

The calculation of $\bar{\boldsymbol{M}}$ is closely analogous to that of the diffusion contribution to the bulk particle stress, carried out by Hinch & Leal (1972) (cf. (2.16) *et seq.*). Upon making use of (1.5) and (3.2*a*), the Cartesian scalar components of $\Delta\hat{\bar{\boldsymbol{M}}}$ are written as

$$(\Delta\hat{\bar{\boldsymbol{M}}})_{ij} = 15(\bar{f}_{ij} - \tfrac{1}{3}\delta_{ij}), \tag{4.4}$$

with $\bar{f}_{ij}$ defined as in (2.25). As with the particle bulk stress, $P_0^{\infty(0)}$ contributes only to the diagonal elements of $\Delta\hat{\bar{\boldsymbol{M}}}$ $[(\Delta\hat{\bar{\boldsymbol{M}}})_{ij}, i=j]$, whereas the correction $P_0^{\infty(1)}$ contributes only to the off-diagonal elements ($i \neq$ j). The eigenvalues of $\Delta\hat{\bar{\boldsymbol{M}}}$ are

$$\nu_i \approx 15\left(\bar{f}_{ii}^{(0)} - \frac{1}{3}\right) + O(Pe^{-2}) \quad (i = 1,2,3), \tag{4.5a–c}$$

whereas the corresponding eigenvectors are

$$\boldsymbol{u}_1 = \left(1, -\frac{\bar{f}_{12}^{(1)}}{\bar{f}_{22}^{(0)} - \bar{f}_{11}^{(0)}} Pe^{-1}, 0\right), \quad \boldsymbol{u}_2 = \left(-\frac{\bar{f}_{12}^{(1)}}{\bar{f}_{22}^{(0)} - \bar{f}_{11}^{(0)}} Pe^{-1}, -1, 0\right), \tag{4.6a, b}$$

$$\boldsymbol{u}_3 = (0,0,1). \tag{4.6c}$$

(The expressions for $\bar{f}_{11}^{(0)}, \bar{f}_{22}^{(0)}, \bar{f}_{33}^{(0)}$ and $\bar{f}_{12}^{(1)}$ can be found elsewhere.†) Thus, when $Pe \to \infty$ the rotation about $-\boldsymbol{i}_3$ of the principal directions of $\bar{\boldsymbol{M}}$, $\boldsymbol{u}_1$ and $\boldsymbol{u}_2$, pointed out in the preceding section (cf. (3.12) *et seq.*), is completed, and $\boldsymbol{u}_1$ becomes aligned with the direction of the undisturbed fluid velocity.

4.3. *The dyadic* **b**-*field*

The scalar Cartesian components b_{ij} satisfy (2.28) and (2.24*b*), which are rewritten here in the respective forms

$$\boldsymbol{\nabla}_e\cdot(\hat{\dot{\boldsymbol{e}}} b_{ij}) - Pe^{-1}\nabla_e^2 b_{ij} = Pe^{-1}\varphi_{ij} + \delta_{i1} b_{2j} \tag{4.7a}$$

and

$$\int_{S_2} b_{ij}\,\mathrm{d}^2\boldsymbol{e} = 0. \tag{4.7b}$$

Following Leal and Hinch (cf. (4.2)), the above equations are supplemented by the integral condition

$$\int_c \mathrm{d}s\,\boldsymbol{\nu}\cdot\boldsymbol{\nabla}_e \boldsymbol{b}_{ij} = -\int_S \varphi_{ij}\,\mathrm{d}^2\boldsymbol{e} + Pe\,\delta_{i1}\int_S b_{2j}\,\mathrm{d}^2\boldsymbol{e}. \tag{4.7c}$$

This is obtained by integration of (4.7*a*) over the domain S lying on the surface of the unit sphere, which is bounded by the Jeffery orbit c, upon taking advantage of the fact that $\boldsymbol{\nu}\cdot\hat{\dot{\boldsymbol{e}}} = 0$ on c. In the foregoing,

$$\varphi_{ij} = P_0^\infty(f_{ij} - \bar{f}_{ij}) \tag{4.8}$$

† Cf. the footnote following (3.4).

(cf. (2.28)). The latter can be represented by the expression

$$\varphi_{ij}(\boldsymbol{e}) \approx \varphi_{ij}^{(0)}(\boldsymbol{e}) + Pe^{-1}\varphi_{ij}^{(1)}(\boldsymbol{e}) + O(Pe^{-2}), \tag{4.9}$$

which suggests that b_{ij} too possesses an asymptotic expansion in descending powers of Peclét number. While φ_{ij} is symmetric by definition, owing to the last term on the right-hand side of (4.7*a*) the single symmetry relation satisfied by b_{ij} is $b_{23} = b_{32}$. In the following we outline the asymptotic calculation of the respective leading-order terms of b_{ij}. Further details as well as calculation of higher-order terms relevant to the subsequent derivation are provided elsewhere.†

When $i \neq 1$, the respective last terms on the right-hand sides of both (4.7*a*) and (4.7*c*) vanish. We therefore assume that

$$b_{ij} \approx b_{ij}^{(0)} + Pe^{-1}b_{ij}^{(1)} + O(Pe^{-2}). \tag{4.10}$$

The problem for $b_{ij}^{(0)}$ possesses a non-trivial solution only if the first term on the right-hand side of (4.7*c*) does not vanish upon substitution of the corresponding $\varphi_{ij}^{(0)}$. Making use of the orbit coordinates (C, τ) one readily concludes from symmetry considerations that the above-mentioned forcing term does vanish when $i \neq j$, hence the relevant b_{ij} satisfy

$$b_{21}^{(0)} = b_{23}^{(0)} = b_{31}^{(0)} = b_{32}^{(0)} = 0. \tag{4.11}$$

For $i = j$, we write the leading-order equation resulting from (4.7*a*) in terms of the orbit coordinates

$$\frac{\partial}{\partial \tau}(g^{-1}b_{ij}^{(0)}) = 0, \tag{4.12}$$

which is readily inverted to yield

$$b_{ij}^{(0)} = \beta_{ij}^{(0)}(c)\, g(C, \tau). \tag{4.13}$$

Appearing in the above are

$$g^{-1}(C, \tau) = \frac{\partial(\theta, \phi)}{\partial(C, \tau)} \sin\theta \tag{4.14}$$

and $\beta_{ij}^{(0)}$ which, as indicated by their respective arguments, are functionally dependent only upon the coordinate C (the orbit parameter). These latter functions are determined via substitution of (4.13) into (4.7*c*) resulting in a linear, first-order, inhomogeneous differential equation which is integrated in conjunction with the normalization condition (4.7*b*).

When $i = 1$, the leading order of b_{ij} depends upon the order of the corresponding b_{2j}. Since $b_{2j} \approx O(Pe^{-1})$ for $j = 1, 3$, it can be verified that the expansion (4.10) together with the expression (4.13) remain appropriate. (Note, however, that $b_{1j}^{(0)}$, $j = 1, 3$, are fully determined only after the corresponding $b_{2j}^{(1)}$ have been calculated.) Finally, since $b_{22} \approx O(1)$, we obtain

$$b_{12} \approx Pe\, b_{12}^{(0)} + b_{12}^{(1)} + O(Pe^{-1}), \tag{4.15}$$

in which $b_{12}^{(0)}$ is again of the form given by (4.13).

Before proceeding to the evaluation of the Taylor dispersivity dyadic, some additional comments regarding the respective asymptotic orders of the scalar components of $\boldsymbol{b}$, as they appear in the foregoing results, seem warranted. As mentioned above (cf. (2.17) *et seq.*) the vector $\boldsymbol{B}$-field represents the long-time limit of the relative position vectors of the respective centroids of the orientation-specific sub-populations (i.e. consisting of individual particles possessing the same instantaneous

† Cf. the footnote following (3.4).

orientation). In the present problem, relative distances of $O(Pe)$ are possible only in the direction $\boldsymbol{i}_1$ of the fluid velocity, and then only as a result of an external force acting in the direction $\boldsymbol{i}_2$ along which fluid velocity changes take place. From the definition (2.23) it is obvious that b_{12} is the only component of $\boldsymbol{b}$ representing the latter combination of directions, and is therefore the only $O(Pe)$ component.

4.4. *Taylor dispersivity*

The dimensionless dyadic $\hat{\boldsymbol{D}}^C$ (3.8*b*) is given in Cartesian tensor notation by

$$\hat{\boldsymbol{D}}_{ij}^C = \tfrac{1}{2}\hat{F}_k\hat{F}_l\int_{S_2}(b_{ik}f_{jl}+b_{jk}f_{il})\,\mathrm{d}^2\boldsymbol{e}, \tag{4.16}$$

in which $\hat{F}_i$ denotes the components of the unit vector $\hat{\boldsymbol{F}}$, and summation over repeated indices is understood. Upon making use of: (i) the foregoing order-of-magnitude estimates for the various b_{ij}; (ii) the fact that in all cases where b_{ij} is at least $O(1)$ the leading-order terms $b_{ij}^{(0)}$ adopt the functional form (4.13); and (iii) utilizing the normalization condition (4.7*b*), we ultimately obtain the eigenvalues of $\hat{\boldsymbol{D}}^C$, satisfying the characteristic equation $|\hat{\boldsymbol{D}}^C-\nu\boldsymbol{I}|=0$, which to the indicated orders are

$$\nu_{1,2}\approx\tfrac{1}{2}Pe\,[d_{11}^C\pm((d_{11}^C)^2+4(d_{12}^C)^2+4(d_{13}^C)^2)^{\frac{1}{2}}]+O(1), \tag{4.17a, b}$$

$$\nu_3\approx\frac{(d_{13}^C)^2\,d_{22}^C+(d_{12}^C)^2\,d_{33}^C-2d_{12}^C\,d_{23}^C\,d_{13}^C}{(d_{12}^C)^2+(d_{13}^C)^2}+O(Pe^{-1}), \tag{4.17c}$$

and the respective eigenvectors

$$\boldsymbol{u}_{1,2}=\left[1,\frac{2d_{12}^C}{d_{11}^C\pm((d_{11}^C)^2+4(d_{12}^C)^2+4(d_{13}^C)^2)^{\frac{1}{2}}},\frac{2d_{13}^C}{d_{11}^C\pm((d_{11}^C)^2+4(d_{12}^C)^2+4(d_{13}^C)^2)^{\frac{1}{2}}}\right] \tag{4.18a, b}$$

and

$$\boldsymbol{u}_3=(0,-d_{13}^C,d_{12}^C). \tag{4.18c}$$

The various scalar elements d_{ij}^C appearing in the above as well as the $O(1)$ scalars $d_{ij}^{(0)}$, $d_{ij}^{(1)}$ and $\hat{B}_{ij}^{(0)}$ appearing in the following are tabulated elsewhere.†

The most notable result here is the occurrence of a *negative* eigenvalue, which is proportional to Pe. The latter result and the above asymptotic estimates remain essentially the same provided that $\hat{\boldsymbol{F}}\cdot\hat{\boldsymbol{G}}\neq\boldsymbol{0}$, i.e. as long as $\hat{\boldsymbol{F}}$ does not belong to the null space of the velocity gradient (Frankel & Brenner 1991). In the present example this requires that $\hat{F}_2\neq 0$. Since $\hat{F}_2$ is the source of the most significant interaction between the 'Taylor mechanism' and the shear field, we focus in the following on the case $\hat{F}_2=1$ ($\hat{\boldsymbol{F}}=\boldsymbol{i}_2$).

The case $F_2 = 1$

Substitute $\hat{F}_1,\hat{F}_3=0$ and make use of (4.16) to obtain the eigenvalues and eigenvectors of $\hat{\boldsymbol{D}}^C$:

$$\nu_{1,2}\approx\pm Pe\,d_{12}^{(0)}+\tfrac{1}{2}(d_{11}^{(1)}+d_{22}^{(1)})+O(Pe^{-1});\quad \nu_3\approx O(Pe^{-2}) \tag{4.19a–c}$$

and

$$\boldsymbol{u}_{1,2}\approx\left(1,\pm1-\frac{1}{2}\frac{d_{11}^{(1)}-d_{22}^{(1)}}{d_{12}^{(0)}}Pe^{-1},0\right);\quad \boldsymbol{u}_3=(0,0,1). \tag{4.20a–c}$$

These show that the initial trends indicated earlier by the solution for $Pe\ll 1$ (cf. (3.13) and (3.14)) are complemented by the latter results, which show that for $Pe\to\infty$ the

† Cf. the footnote following (3.4).

principal directions of $\hat{\boldsymbol{D}}^C$ coincide with those of $\hat{\boldsymbol{S}}$. That the negative eigenvalue of $\hat{\boldsymbol{D}}^C$ is associated with the principal direction of contraction in the shear field is a very gratifying result, as it appears to support the conjecture of the general theory (Frankel & Brenner 1991, §5) that the non-positive nature of $\hat{\boldsymbol{D}}^C$ is due to the inseparable coupling that exists between the Taylor dispersion mechanism and the (deterministic) distortion arising from the shear field.

4.5. *Modified Taylor dispersivity*

From (2.11*a*) in conjunction with (2.9) and (2.23) one obtains

$$\hat{\bar{\boldsymbol{D}}}^C = \hat{\boldsymbol{D}}^C + Pe\,\hat{\boldsymbol{B}}, \tag{4.21a}$$

where

$$\hat{\boldsymbol{B}} \stackrel{\text{def}}{=} \left[\!\!\left[\int_{S_2} \frac{1}{P_0^\infty} (\boldsymbol{b}\cdot\hat{F})(\boldsymbol{b}\cdot\hat{F})\, \mathrm{d}^2\boldsymbol{e}\cdot\hat{\boldsymbol{G}} \right]\!\!\right]^s. \tag{4.21b}$$

We focus in the following on the above example and substitute $\boldsymbol{F} = \boldsymbol{i}_2$ together with $\hat{\boldsymbol{G}}$ corresponding to simple shear, (3.10), to obtain the scalar components of the dyadic $\hat{\boldsymbol{B}}$. Substitute these, together with the corresponding elements of $\hat{\boldsymbol{D}}^C$ into (4.21*a*) and solve the characteristic equation $|\hat{\bar{\boldsymbol{D}}}^C - \nu\boldsymbol{I}| = 0$ to obtain the eigenvalues

$$\nu_1 \approx Pe^2\,\hat{B}_{11}^{(0)} + O(1), \tag{4.22a}$$

$$\nu_2 \approx d_{22}^{(1)} - \frac{d_{12}^{(0)} + \hat{B}_{12}^{(0)}}{\hat{B}_{11}^{(0)}} [d_{12}^{(0)} + \hat{B}_{12}^{(0)} + 2Pe^{-1}\, d_{12}^{(1)}] + O(Pe^{-2}), \tag{4.22b}$$

$$\nu_3 \approx O(Pe^{-2}), \tag{4.22c}$$

as well as the corresponding eigenvectors

$$\boldsymbol{u}_1 \approx \left[1, \frac{d_{12}^{(0)} + \hat{B}_{12}^{(0)}}{\hat{B}_{11}^{(0)}} Pe^{-1}, O(Pe^{-3})\right], \quad \boldsymbol{u}_2 \approx \left[\frac{d_{12}^{(0)} + \hat{B}_{12}^{(0)}}{\hat{B}_{11}^{(0)}} Pe^{-1}, -1, O(Pe^{-2})\right], \tag{4.23a, b}$$

$$\boldsymbol{u}_3 \approx [O(Pe^{-3}), O(Pe^{-2}), 1]. \tag{4.23c}$$

Comparison of these latter results with those for $\hat{\boldsymbol{D}}^C$, (4.19) and (4.20), respectively, reveals that the pair of $O(Pe)$ eigenvalues of $\hat{\boldsymbol{D}}^C$, corresponding to the principal directions of $\hat{\boldsymbol{S}}$ in the plane of the flow, are here replaced by an eigenvalue which grows like Pe^2 and another one which, for $Pe \to \infty$, tends to a constant value (independent of Pe), corresponding, respectively, to the direction of the undisturbed flow and the direction perpendicular thereto.

5. Dispersion in simple shear; arbitrary Peclét numbers ($Pe = O(1)$)

The case of arbitrary Peclét numbers, where the respective effects of shear and rotary diffusion are of comparable importance, is studied in this section by representing the fields P_0^∞ and $P_0^\infty \boldsymbol{B}$ (i.e. $\boldsymbol{b}$) by series expansions of surface spherical harmonics and computing the coefficients appearing therein by means of appropriate numerical routines.

5.1. *The field P_0^∞*

Owing to the fore–aft symmetry of the particles, P_0^∞ is necessarily invariant under the transformation $\boldsymbol{e} \to -\boldsymbol{e}$. When $\boldsymbol{e}$ is parameterized in terms of the Eulerian angles (θ, ϕ), this invariance is expressed by the condition

$$P_0^\infty(\pi - \theta, \phi + \pi) = P_0^\infty(\theta, \phi). \tag{5.1}$$

Additionally, it is readily verified that the problem posed by (2.21) and (2.27) admits a solution which is symmetric about $\theta = \frac{1}{2}\pi$, so that

$$P_0^\infty(\pi-\theta,\phi) = P_0^\infty(\theta,\phi), \tag{5.2}$$

as well as being symmetric about $\phi = \pi$ (the latter being a consequence of (5.1) and (5.2)). Thus, P_0^∞ may be represented by the series

$$P_0^\infty = \sum_{n=0}^{\infty}\left\{\tfrac{1}{2}A_n P_{2n}(\cos\theta) + \sum_{m=1}^{n}(A_n^m\cos 2m\phi + B_n^m \sin 2m\phi)\,P_{2n}^{2m}(\cos\theta)\right\}, \tag{5.3}$$

which is restricted to even orders and degrees so as to satisfy both of the above symmetry conditions.

Following Stewart & Sorensen (1972), P_0^∞ is approximated by Galerkin's method. To this end, the series expansion (5.3) is truncated beyond some finite value $n = N$ so as to obtain the approximation $P_0^{\infty(N)}$. The left-hand side of (2.21*a*) is then rendered orthogonal to all surface harmonics of degree $n \leqslant N$. Use of orthogonality properties and recursive relations satisfied by the associated Legendre functions P_{2n}^{2m} leads to a linear system of N^2+2N algebraic equations for the coefficients A_n, A_n^m and B_n^m ($n = 1,2,\ldots,n$; A_0 is determined from the normalization condition (2.21*b*)).

5.2. *The **B**-field*

Apart from satisfying a fore–aft symmetry condition analogous to (5.1), b_{ij} satisfies an additional requirement depending upon the symmetry properties of the respective forcing terms (cf. (2.28)). When $i,\ j \neq 3$ or $i=j=3$, the latter terms allow the additional condition (5.2); hence, b_{ij} is represented by the expansion

$$b_{ij} = \sum_{n=0}^{\infty}\left\{\tfrac{1}{2}c_n^{(ij)} P_{2n}(\cos\theta) + \sum_{m=1}^{n}[c_n^{(ij)\,m}\cos 2m\phi + D_n^{(ij)\,m}\sin 2m\phi]\,P_{2n}^{2m}(\cos\theta)\right\}$$
$$(i,j \neq 3 \text{ or } i=j=3), \tag{5.4}$$

in which, similarly to (5.3), both the orders and degrees are restricted to even values. When $i = 3$ or $j = 3$ ($i \neq j$), the forcing terms are odd with respect to $\theta = \frac{1}{2}\pi$ (as well as with respect to $\phi = \pi$), i.e.

$$b_{ij}(\pi-\theta,\phi) = -b_{ij}(\theta,\phi). \tag{5.5}$$

Inasmuch as the degrees must be even in order to satisfy (5.1), the orders are here restricted to odd values; consequently,

$$b_{ij} = \sum_{n=1}^{\infty}\sum_{m=1}^{n}[E_n^{(ij)\,m}\cos((2m-1)\phi) + F_n^{(ij)\,m}\sin((2m-1)\phi)]\,P_{2n}^{2m-1}(\cos\theta)$$
$$(i = 3 \text{ or } j = 3;\ i \neq j). \tag{5.6}$$

The computational procedure employed is similar to that employed when calculating P_0^∞. The approximation $P_0^{\infty(N)}$ enables one to obtain the (approximate) forcing terms on the right-hand side of (2.28) up to $n = N-1$. Substitution of (5.4), truncated beyond $n = N-1$, into (2.28) yields a linear system of N^2-1 equations for C_n, C_n^m and D_n^m ($n = 1,2,\ldots,N-1$; $m = 1,2,\ldots,n$; with $C_0 = 0$ by (2.24*b*)). From (5.6), we similarly obtain a system of $N(N-1)$ linear algebraic equations for E_n^m and F_n^m ($n = 1,2,\ldots,N-1$; $m = 1,2,\ldots,n$). The respective systems for the various b_{ij} can be solved recursively; however, one has to obtain b_{2j} prior to calculating b_{1j} since the former appears in the forcing term of the latter (cf. (2.28)).

5.3. *Average translational mobility and Taylor dispersivity*

Substitute P_0^∞ from (5.3) into the definition (2.8*b*) of $\hat{\boldsymbol{M}}$ in conjunction with (1.5) to obtain $\Delta\hat{\boldsymbol{M}}$ (cf. (3.2*a*)). The results indicate that the degree of anisotropy, $\Delta\hat{\boldsymbol{M}}$, of the average mobility depends only upon the lowest-order coefficients (of P_2 and P_2^2) in the series expansion (5.3) of P_0^∞. This fact could have been anticipated in view of the orthogonality property (3.6), since the variable portion of $\boldsymbol{M}$, cf. (1.5), is proportional to the dyadic surface spherical harmonic $\boldsymbol{P}_2$.

Substitution of the appropriate series expansion for b_{ij} (either (5.4) or (5.6)) into (4.16) followed by integration yields the components of $\hat{\boldsymbol{D}}^C$ (explicit expressions of which together with those pertaining to the above $\Delta\hat{\boldsymbol{M}}$ are omitted here†). As in the case of $\Delta\hat{\boldsymbol{M}}$, $\hat{\boldsymbol{D}}^C$ depends only upon the lowest-order coefficients of P_2, P_2^1 and P_2^2 appearing in the respective expansions of b_{ij}. This accords with the orthogonality property (3.6) together with the expression (3.8*b*).

6. Results and discussion

When normalized with respect to $\frac{1}{3}(M_\parallel + 2M_\perp)$, the (dimensionless) average mobility is (cf. (3.2*a*))

$$\hat{\boldsymbol{M}} = \boldsymbol{I} + \boldsymbol{\delta}^M. \tag{6.1}$$

Similarly, normalization of $\boldsymbol{D}^*$ with respect to $\frac{1}{3}kT(M_\parallel + 2M_\perp)$ yields the dimensionless relation (cf. (2.9) and (3.8*a*))

$$\hat{\boldsymbol{D}}^* = \hat{\boldsymbol{M}} + \boldsymbol{\delta}^C, \tag{6.2a}$$

in which

$$\boldsymbol{\delta}^C = \frac{3(M_\parallel - M_\perp)^2 F^2}{kT(M_\parallel + 2M_\perp)\, d_r} \hat{\boldsymbol{D}}^C. \tag{6.2b}$$

As pointed out in connection with (3.2*a*), $\boldsymbol{\delta}^M$ represents the departure of the average mobility from the isotropic result corresponding to sedimentation in a quiescent fluid, while $\boldsymbol{\delta}^C$ represents the contribution to the dispersivity arising from the Taylor dispersion mechanism. In this section we study the functional dependence of $\boldsymbol{\delta}^M$ and $\boldsymbol{\delta}^C$ upon the magnitude of the shear rate and the geometry of the particles (in particular their deviation from a spherical shape). Explicit results are presented in what follows for spheroidal particles, for which the equivalent axis ratio r is simply the ratio between their respective polar and equatorial radii.

Making use of expressions existing in the literature (e.g. Brenner 1974) for λ, $M_\parallel$, $M_\perp$ and d_r, one obtains

$$\lambda = \frac{r^2-1}{r^2+1}, \quad \frac{M_\parallel - M_\perp}{M_\parallel + 2M_\perp} = \frac{2\gamma r^2 + \gamma - 3}{8\gamma(r^2-1)} \tag{6.3a, b}$$

and

$$\frac{3(M_\parallel - M_\perp)^2 F^2}{kT(M_\parallel + 2M_\perp)\, d_r} = \frac{1}{8}\left(\frac{r^2+1}{r^2-1}\right)\frac{(2\gamma r^2+\gamma-3)^2}{\gamma r^{\frac{4}{3}}(2\gamma r^2-\gamma-1)}\left(\frac{F\ell}{kT}\right)^2. \tag{6.3c}$$

In the foregoing,

$$\gamma = \begin{cases} \dfrac{\cosh^{-1} r}{r(r^2-1)^{\frac{1}{2}}} & \text{for a prolate spheroid} \quad (1 \leqslant r < \infty) \\[2ex] \dfrac{\cos^{-1} r}{r(1-r^2)^{\frac{1}{2}}} & \text{for an oblate spheroid} \quad (0 < r \leqslant 1). \end{cases} \tag{6.4}$$

† Cf. the footnote following (3.4).

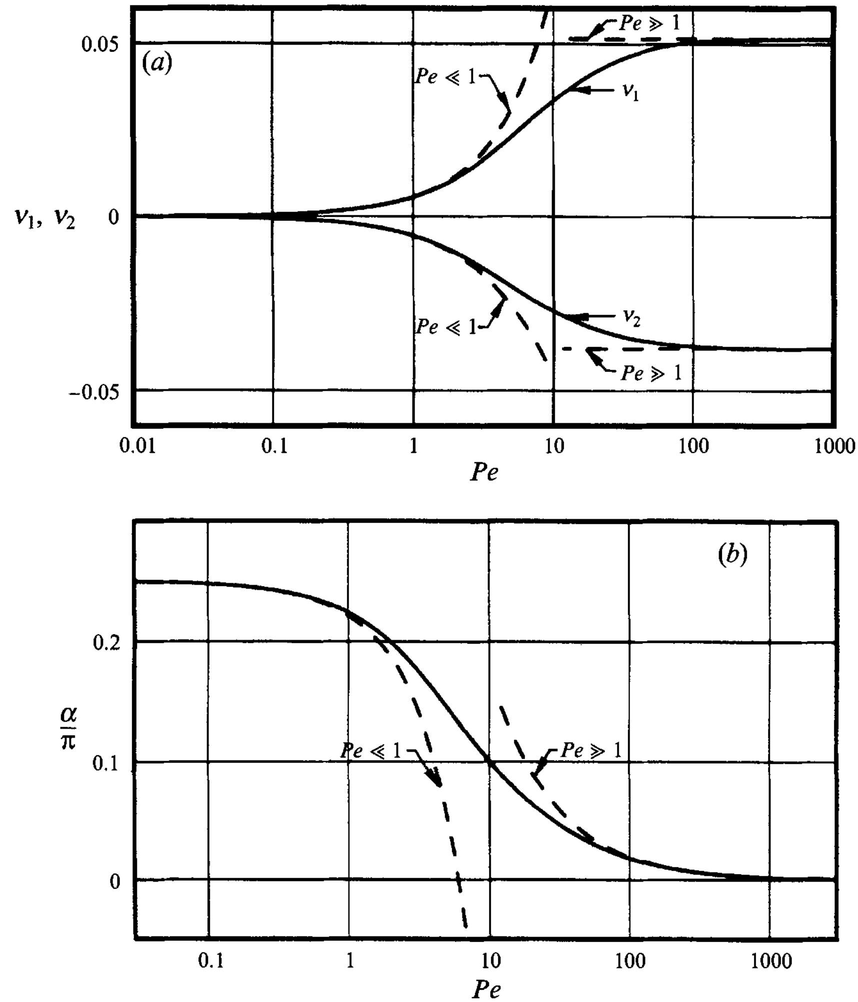

FIGURE 2. Variation of $\mathbf{\delta}^M$, the anisotropic portion of the dimensionless average mobility, with rotary Peclét number for a prolate spheroid of axis ratio $r = 3$. ——, Exact solution, (§5.3); ----, $Pe \ll 1$, (3.11) and (3.12), and $Pe \gg 1$, (4.5) and (4.6), approximations. (*a*) The eigenvalues ν_1 and ν_2 corresponding to principal directions in the plane (x, y) of the simple shear flow. (*b*) The angle α between the principal direction associated with ν_1 and the direction of the undisturbed fluid velocity.

Moreover, ℓ, appearing in the Langevin parameter $\chi = F\ell/kT$, is the 'equivalent' radius of the spheroid (i.e. the radius of an equal-volume sphere).

In each of the following figures the upper portion, (*a*), describes the variation of the pair of eigenvalues ν_1 and ν_2 corresponding to the principal directions in the plane of the simple shear flow of the relevant dyadic, whereas the lower portion, (*b*), shows the variation of the angle α which one (specified) of these principal directions makes with the direction $\boldsymbol{i}_1$ of the undisturbed fluid velocity.

Figure 2 describes the dependence of $\mathbf{\delta}^M$ upon Pe for a prolate spheroid of axis ratio $r = 3$. The solid lines correspond to the exact solution (§5.3) while the dashed lines represent, respectively, the small-Peclét-number, (3.11) and (3.12), and large-Peclét-number, (4.5) and (4.6), asymptotes. In part (*a*) we see that the absolute values of both ν_1 (> 0) and ν_2 (< 0) grow monotonically from $\nu_1, \nu_2 = 0$ at $Pe = 0$ (corresponding to an isotropic average mobility) to the respective constant limits $\nu_1 = 5.15 \times 10^{-2}$ and $\nu_2 = -3.81 \times 10^{-2}$ predicted by (4.5) for $Pe \rightarrow \infty$. Part (*b*) shows that the angle α which the eigenvector associated with ν_1 makes with the fluid velocity decreases monotonically from $\alpha = \frac{1}{4}\pi$ (the principal direction of strain) for $Pe \rightarrow 0$ (cf. (3.2*b*) and (3.12) *et seq.*) to the limit $\alpha = 0$ for $Pe \rightarrow \infty$.

Since for a prescribed value of r the average mobility is determined by $P_0^{\infty}(\boldsymbol{e})$, the foregoing trends can be explained in terms of the variation with Pe of the orientational 'equilibrium' distribution. The latter begins as a uniform distribution for $Pe = 0$, becomes proportional to the strain rate $\hat{\boldsymbol{S}}$ for $Pe \ll 1$, (3.1), and reaches a constant (independent of Pe) limiting distribution, $P_0^{\infty(0)}(\boldsymbol{e})$, in the limit $Pe \rightarrow \infty$, (4.3). According to Leal & Hinch (1971), with increasing $Pe\,(\gg 1)$, prolate particles tend to spend an increasing portion of their rotational trajectory time along (most of) Jeffery's orbits, being nearly aligned with the flow. When this is considered in conjunction with the fact that the mobility of a prolate spheroid is largest (smallest) in the axial (transverse) direction, one anticipates a monotonic increase in the positive increment of the slip velocity (of the particle centre relative to the approaching fluid), represented by ν_1 tending, for $Pe \rightarrow \infty$, to a constant maximal value in the direction of the flow. The accompanying deficit in the slip velocity (represented by $\nu_2 < 0$) will likewise increase to a constant limit in the direction $\boldsymbol{i}_2$, perpendicular to the undisturbed fluid velocity.

Figure 3 shows the variation of $\boldsymbol{\delta}^C$ with Pe for a prolate particle with $r = 3$. The solid lines are obtained from the exact solution (§5.3) while the broken lines represent the respective approximate solutions for $Pe \ll 1$, (3.13) and (3.14), and $Pe \gg 1$, (4.19) and (4.20). In part (*a*) we see that both eigenvalues start from the values corresponding to sedimentation in a quiescent fluid. The larger one, ν_1, grows slowly, passes through a (shallow) maximum (at $Pe \approx 2$) followed by a minimum (at $Pe \approx 50$) and then rises monotonically. The other eigenvalue, ν_2, decreases monotonically, becoming negative for $Pe > 40$. For large Peclét numbers both curves become mirror images of each other, and the absolute values of ν_1 and ν_2 grow linearly with Pe (cf. (4.19)). (The growth looks exponential because of the logarithmic scale selected for Pe.) The angle α in part (*b*) of the figure corresponds to the principal direction associated with ν_2, the eigenvalue which becomes ultimately negative. The curve starts from $\alpha = 0$, i.e. perpendicular to the external force ($\hat{\boldsymbol{F}} = \boldsymbol{i}_2$), which agrees with the result for sedimentation in the absence of shear. The angle α then decreases to a minimal value $\alpha \approx -0.4\pi$ at $Pe \approx 11$, goes through a shallow maximum (at $Pe \approx 125$), and finally converges to the asymptotic value $\alpha = -\frac{1}{4}\pi$, i.e. parallel to the principal direction of contraction in the shear field.

As noted above (cf. (4.20) *et seq.*), this result provides an important insight which helps resolve the following 'riddle' in the general theory (Frankel & Brenner 1991): adoption of the codeformational view via the application of the Oldroyd derivative in (2.7) should presumably eliminate the (deterministic) contributions of the shear flow to the rate of spread, thereby rendering $\boldsymbol{D}^C$ positive definite; as the foregoing results demonstrate, this is evidently not the case. Frankel & Brenner show that the rate of spread embodied in $\boldsymbol{D}^C$ is determined not only by the instantaneous velocities of the solute particles, but depends upon their instantaneous configuration in physical space as well. In this configuration, which is an outcome of the past evolution of the 'cloud' of particles, the respective effects of the Taylor dispersion mechanism and the (deterministic) distortion in the shear field, are inseparably coupled. In this respect, the latter result – which relates the non-positive nature of $\boldsymbol{D}^C$ to the contraction in the shear flow – is a very gratifying one, as it provides clear evidence (in a well-defined physical context) in support of the abstract explanations previously given.

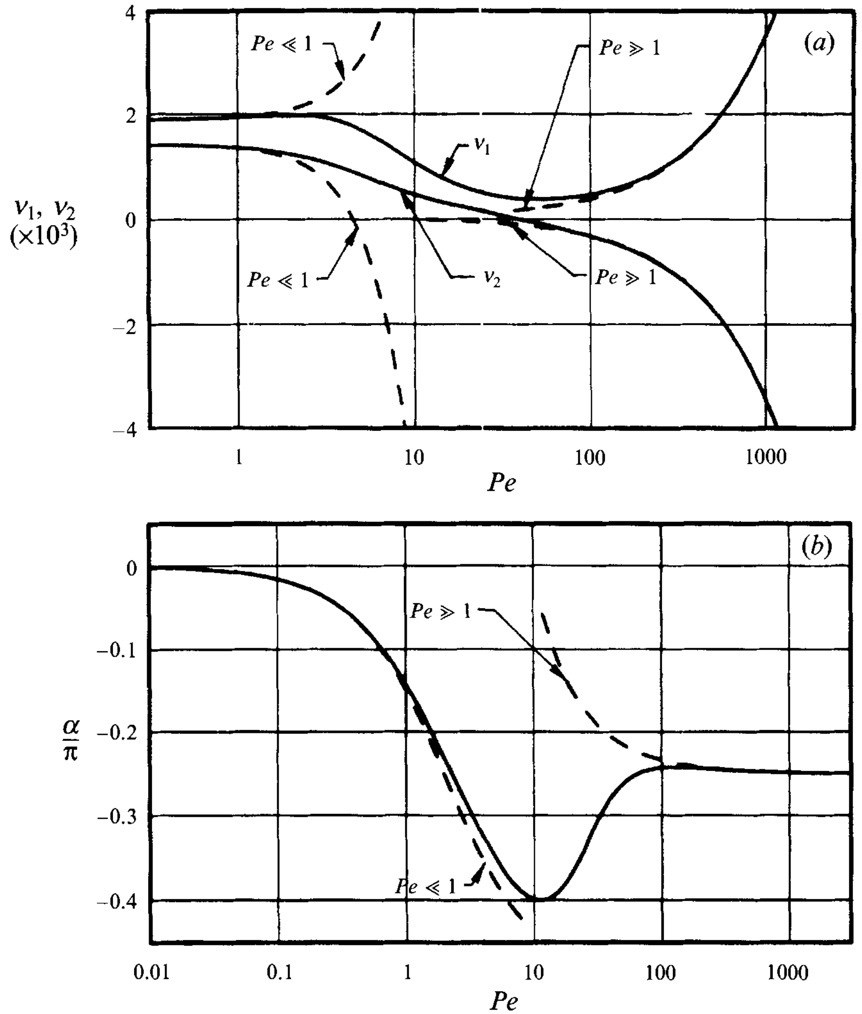

FIGURE 3. Variation of $\mathbf{\delta}^C$, the dimensionless Taylor dispersivity, with the rotary Peclét number for a prolate spheroid of axis ratio $r = 3$. ——, Exact solution, (§5.3); ------ $Pe \ll 1$, (3.13) and (3.14), and $Pe \gg 1$, (4.19) and (4.20), approximations. (*a*) The eigenvalues ν_1 and ν_2 corresponding to principal directions in the plane (x, y) of the simple shear flow. (*b*) The angle α between the principal direction associated with ν_2 and the direction of the undisturbed fluid velocity.

Comparison of the exact and asymptotic solutions presented thus far reveals that the asymptotic solution based on the assumption $Pe \ll 1$ is, in fact, a good approximation up to $Pe \approx 1$ (and even slightly beyond). On the other hand, the large-Peclét-number approximation becomes quantitatively valuable only for $Pe \approx 200$. Both observations are now explained. The $Pe \ll 1$ approximation actually presumes that the various quantities calculated are slowly varying functions of Pe, and can therefore be described by including only a small number of terms in a Taylor series expansion. The exact solution verifies that this is indeed the case for both $\Delta\hat{\mathbf{M}}$ and $\hat{\mathbf{D}}^C$ up to $Pe \approx 1$. On the other hand, the $Pe \gg 1$ calculation is based on the assumption that the effect of Brownian rotation is weak relative to the convective effect of shear throughout the entire orientation space. As mentioned in the footnote appearing at the beginning of §4, Hinch & Leal (1972) showed this assumption to be valid only in circumstances

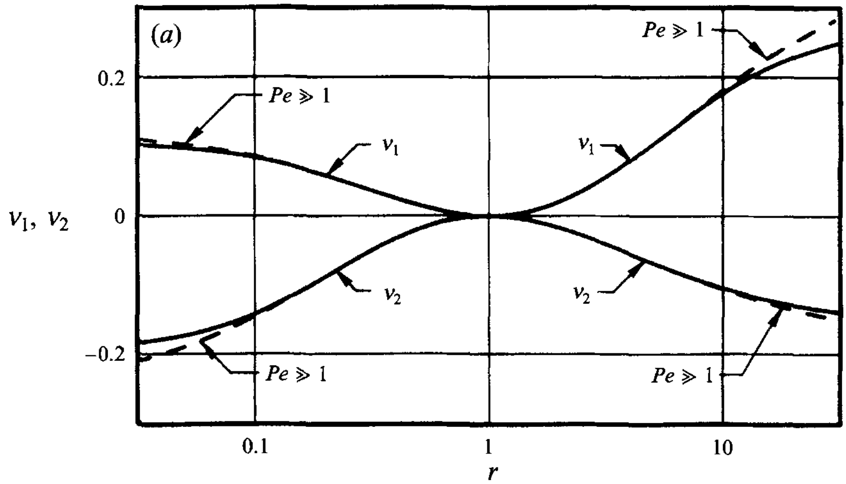

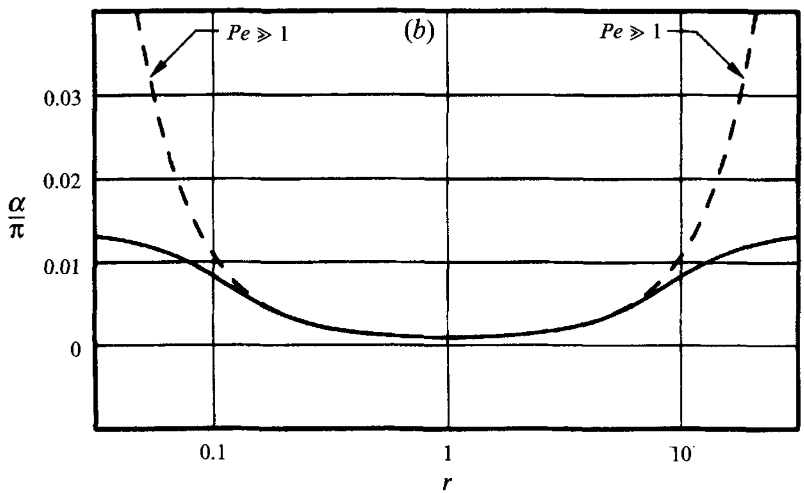

FIGURE 4. Variation of $\mathbf{\delta}^M$, the anisotropic portion of the dimensionless average mobility, with r, the spheroid axis ratio, for $Pe = 1000$. —— Exact solution, (§5.3); ------ $Pe \gg 1$ approximation, (4.5) and (4.6). (*a*) The eigenvalues ν_1 and ν_2 corresponding to the principal directions in the plane (x, y) of the simple shear flow. (*b*) The angle α between the principal direction associated with ν_1 and the direction of the undisturbed fluid velocity.

where the stronger requirement $Pe \gg r^3 + r^{-3}$ is satisfied. It is thus not surprising that in the present example ($r = 3$), the asymptotic solution becomes inaccurate when $Pe < 100$.

The next two figures indicate the influence of particle geometry (i.e. r) upon the average mobility and dispersivity for the case of large Peclét numbers (specifically, $Pe = 1000$). An auxiliary goal is to examine the dependence upon r of the quality of the approximations previously obtained in §4.

Figure 4 describes the variation of $\mathbf{\delta}^M$ with r for $Pe = 1000$. The solid lines are obtained from the exact solution (§5.3), while the broken lines correspond to the $Pe \gg 1$ approximation, (4.5) and (4.6), respectively. Part (*a*) shows that the absolute values of both ν_1 and ν_2 grow monotonically with increasing deviation of the particle from a spherical shape, $r = 1$. (Obviously for $r = 1$, ν_1, $\nu_2 = 0$ because the average mobility is always isotropic for a sphere.) This behaviour results from the increasing difference between the axial, $M_{\|}$, and transverse, $M_{\perp}$, mobilities, in conjunction with the tendency (cf. Hinch & Leal 1972) of the orientational distribution to become increasingly peaked about an orientation nearly aligned with (perpendicular to) the fluid velocity for rod-like (disk-like) particles. In both cases this means that the particles spend an increasing portion of their time in an orientation which favours a slip velocity parallel to the flow. This is manifested by an increasing increment to the average mobility in the direction of the flow accompanied by an increasing deficit in the direction perpendicular thereto. From (6.3*b*) in conjunction with (6.4), it is readily verified that the relative mobility difference is bounded by

$$\lim_{r\to(0,\,\infty)} \frac{M_{\|}-M_{\perp}}{M_{\|}+2M_{\perp}} = (-\tfrac{1}{8}, \tfrac{1}{4}),\ \text{respectively}, \tag{6.5}$$

whence ν_1 and ν_2 are bounded (from above and below, respectively) by $(\frac{1}{2}, -\frac{1}{4})$ for rod-like $(r\to\infty)$ and by $(\frac{1}{8}, -\frac{1}{4})$ for disk-like $(r\to 0)$ spheroids. Part (*a*) of the figure shows that while both ν_1 and ν_2 have not yet reached the above bounds (neither at $r = 0.03$ nor at $r = 30$), they are closer to convergence at the former end of the scale. This observation accords with the faster convergence of the relative mobility difference to the limit (6.5) for oblate spheroids (like $O(r)$ when $r\to 0$) than for prolate spheroids (only like $O(1/\log r)$ when $r\to\infty$).

In figure 4(*b*) we see that, for a wide range of r-values, the principal direction associated with ν_1, the positive eigenvalue, is close to the direction of the undisturbed fluid velocity, in a slightly 'pre-aligned' orientation (e.g. for $\frac{3}{4} \leqslant r \leqslant \frac{4}{3}$, $\alpha \leqslant \pi/1000$). This slight deviation towards the 'pre-aligned' orientation was explained by Hinch & Leal (1972) as a result of the dynamic balance between the convective rotation of the particles, which is biased towards the post-aligned direction, and the diffusive rotary flux down orientational gradients, which acts equally in both pre- and post-aligned directions. It is thus to be expected (and indeed evident in the figure) that the magnitude of the 'pre-alignment' deviation will increase with increasing departure from spherical shape as a consequence of the stronger diffusive influence accompanying the steepening of orientational gradients in the vicinity of the velocity direction.

There is a high degree of similarity between the $r > 1$ and $r < 1$ portions of figure 4; the curves in part (*a*) are nearly skew symmetric, whereas part (*b*) is symmetric with respect to $r = 1$. This similarity stems from the invariance of P_0^{∞} under the transformation

$$r\to 1/r, \quad \theta\to\theta, \quad \phi\to\tfrac{1}{2}\pi+\phi$$

(cf. Leal & Hinch 1971). Since $\Delta\hat{\boldsymbol{M}}$ depends exclusively upon P_0^{∞}, the differences in $\boldsymbol{\delta}^M$ arise only because of the differences in sign and magnitude of the scalar coefficient of the relative mobility difference. These differences affect the eigenvalues ν_1 and ν_2, but not the principal directions of the average mobility deviation.

Figure 5 illustrates the functional dependence of $\boldsymbol{\delta}^C$, the (dimensionless) Taylor dispersivity dyadic, upon the axis ratio r for $Pe = 1000$ according to the exact solution (§5.3, solid lines) and the $Pe \gg 1$ asymptotic solution ((4.19) and (4.20), dashed lines). The latter is seen to provide a good approximation over the range $\frac{1}{5} \leqslant r \leqslant 5$, which, for $Pe = 1000$, is consistent with the requirement $Pe \gg r^3 + r^{-3}$.

Part (*a*) of the figure shows that the absolute values of both ν_1 and ν_2 initially increase with increasing deviation from spherical shape and attain respective maxima at $r \approx 0.3$ and 2.5. With further increased deviation, the foregoing absolute values decrease with increasing differences (first quantitative and later qualitative as well) between the asymptotes and the exact solutions: while the former decrease monotonically and

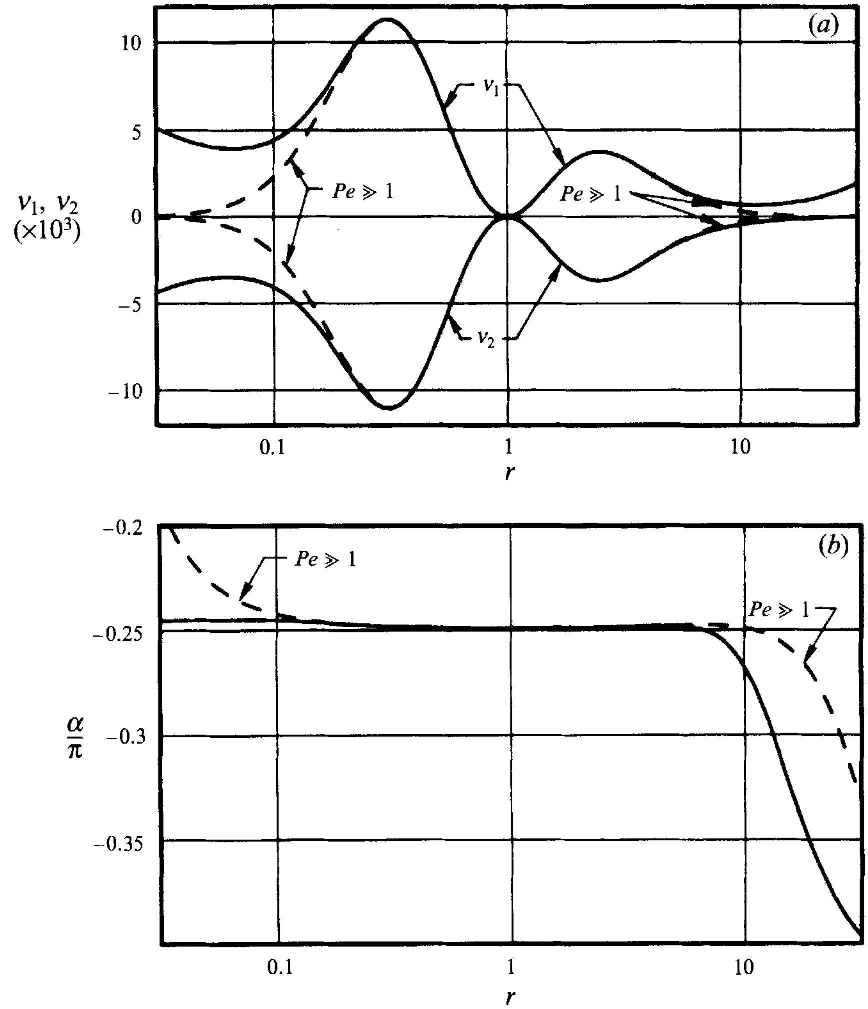

FIGURE 5. Variation of δ^C, the dimensionless Taylor dispersivity, with r, the spheroid axis ratio, for $Pe = 1000$. ——, Exact solution, (§5.3); ------, $Pe \gg 1$ approximation, (4.19) and (4.20). (a) The eigenvalues ν_1 and ν_2 corresponding to principal directions in the plane (x, y) of the simple shear flow. (b) The angle α between the principal direction associated with ν_2 and the direction of the undisturbed fluid velocity.

practically vanish at both ends of the r-scale, the exact solutions (with a single exception) pass through respective minima (at $r \approx 0.06$ and 11) and then resume growth. Figure 5(b), for the angle α between the principal direction associated with the smaller eigenvalue ν_2 and the fluid velocity, shows a wide plateau, where $\alpha \approx \frac{1}{4}\pi$, followed by a rapid decrease for $r > 6$.

The extrema pattern of figure 5(a) results from the balance between two competing mechanisms associated with the increasing departure from a spherical shape.

(i) With increasing $r > 1$ or decreasing $r < 1$, mobility differences between the axial and transverse directions increase, while the rotary diffusivity decreases, resulting in (an unbounded) growth of the scalar coefficient multiplying the dyadic $\hat{\boldsymbol{D}}^C$ in (6.2b). These are analogous in the context of the classical Taylor dispersion tube-flow problem (Taylor 1953), to the enhancement of longitudinal dispersivity accompanying an increase in fluid velocity or a decrease in cross-sectional diffusion, respectively.

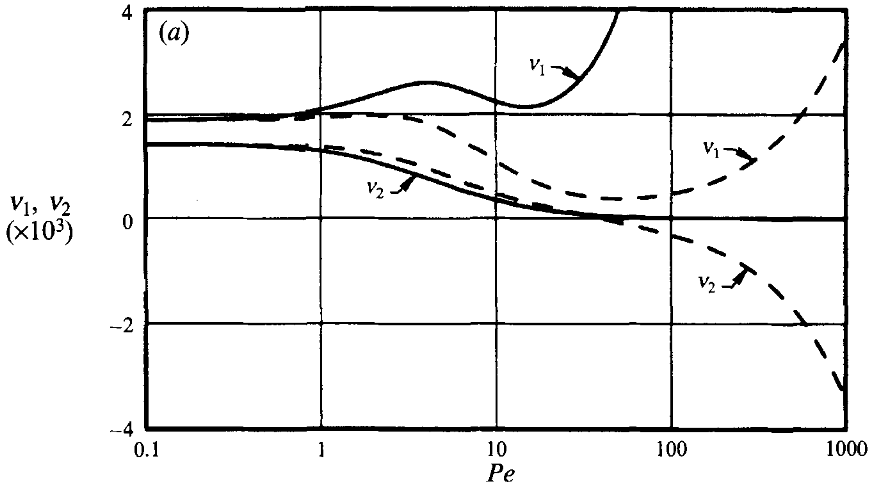

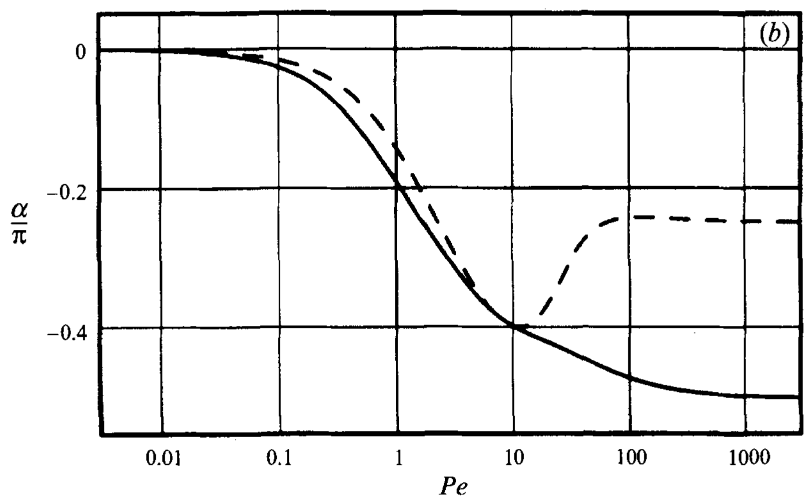

FIGURE 6. Comparison of $\bar{\boldsymbol{\delta}}^C$ and $\boldsymbol{\delta}^C$ for a prolate spheroid of axis ratio $r = 3$. ——, Dimensionless modified Taylor dispersivity, $\bar{\boldsymbol{\delta}}^C$; ------, dimensionless Taylor dispersivity, $\boldsymbol{\delta}^C$ (a) The eigenvalues ν_1 and ν_2 corresponding to principal directions in the plane (x, y) of the simple shear flow. (b) The angle α between the principal direction associated with ν_2 and the direction of the undisturbed fluid velocity.

(ii) As was pointed out previously (cf. the comment at the conclusion of §4.3), the main contribution to $\hat{\boldsymbol{D}}^C$ in the present example, $\hat{\boldsymbol{F}} = \boldsymbol{i}_2$, originates from the fluctuations in the $\boldsymbol{i}_2$-component of the slip velocity coupled with the simple shear flow (in the $\boldsymbol{i}_1$-direction). Therefore, a counteractive influence is associated with the orientational distribution becoming more and more sharply peaked, effectively confining the particles to an increasingly narrower domain about a certain orientation. Furthermore, this particular orientation corresponds to a minimum of the slip-velocity component in the direction of $\hat{\boldsymbol{F}}$ and a concomitant vanishing orientational gradient of this velocity component. (Use (1.5) to obtain

$$\nabla_e(\boldsymbol{U} \cdot \hat{\boldsymbol{F}}) = 2(M_{\parallel} - M_{\perp})(\boldsymbol{e} \cdot \hat{\boldsymbol{F}})(\boldsymbol{I} - \boldsymbol{ee}) \cdot \hat{\boldsymbol{F}} = 0$$

for either $\boldsymbol{e} \cdot \hat{\boldsymbol{F}} = 0$ (rod-like particles) or $\boldsymbol{e} = \hat{\boldsymbol{F}}$ (disk-like particles).) This, in turn, minimizes the $\boldsymbol{i}_2$-velocity differences accompanying the Brownian orientation fluctuations. Thus, the present reduction is comparable in the classical Taylor problem to the decrease in longitudinal dispersion brought about through the restriction of the lateral motion of solute particles to a small portion of the duct cross-sectional area centred about a point of an extremum in the longitudinal fluid velocity.

Figure 5(*a*) thus reveals that with increasing deviation from a spherical shape, it is initially the former effect which prevails. With a further departure from spherical shape, the latter effect dominates, with the former eventually taking over again. Failure of the asymptotic analysis to predict the latter change arises from its inability to account properly for the influence of rotary Brownian diffusion in the so-called singular 'intermediate domain' (where Pe is no longer large compared with r^3+r^{-3}). In reality, by limiting the magnitude of the orientational gradients adjacent to the peak of the orientational probability distribution, this diffusive influence is capable of effectively putting an end to the process of narrowing the probability peak – in turn, enabling the renewed dominance of mechanism (i) over (ii), demonstrated by the occurrence of the minima towards both right and left margins of the figure.

Finally, figure 6 compares the dependence upon Pe of $\boldsymbol{\delta}^C$, the Taylor dispersivity (dashed lines; solid lines in figure 3) and $\bar{\boldsymbol{\delta}}^C$, the modified Taylor dispersivity (solid lines), respectively, of a particle whose axis ratio is $r=3$. (The relation between $\bar{\boldsymbol{\delta}}^C$ and $\bar{\boldsymbol{D}}^C$ is the same as (6.2*b*) defining $\boldsymbol{\delta}^C$ in terms of $\hat{\boldsymbol{D}}^C$.) At small Peclét numbers the respective curves of both families coincide in accordance with the fact that $\boldsymbol{D}^C=\bar{\boldsymbol{D}}^C$ for $Pe=0$ (cf. (2.11*b*)). The upper part (*a*) of the figure shows that with increasing Peclét number the behaviour of the respective larger eigenvalues, ν_1, is qualitatively similar, going initially through a maximum, then a minimum and, finally, diverging monotonically. The ultimate divergence of $\bar{\boldsymbol{D}}^C$ is, however, much faster than that of $\boldsymbol{D}^C$, in accordance with the asymptotic result (4.22*a*) predicting a Pe^2-like growth, as opposed to the linear growth prediction of (4.19*a*). The other eigenvalue, ν_2, of $\bar{\boldsymbol{\delta}}^C$ decreases monotonically; but, unlike the case of $\boldsymbol{\delta}^C$, it remains positive. (In accordance with the asymptotic prediction (4.22*b*), when $Pe\rightarrow\infty$, $\nu_2\rightarrow\nu_2^\infty>0$. The limit ν_2^∞ turns out to be a small number; thus, the scale of the figure makes it appear as though $\nu_2\rightarrow 0$.) Figure 6(*b*) displays the variation with Pe of the principal direction associated with ν_2. Initially (up to $Pe\approx 10$), both curves descend fairly close to each other. The curve corresponding to $\bar{\boldsymbol{\delta}}^C$ continues to descend monotonically, approaching the limiting value $\alpha=-\frac{1}{2}\pi$. The other principal direction, corresponding to the larger eigenvalue, $\nu_1\approx O(Pe^2)$, will thus coincide at large Peclét numbers with the direction of the undisturbed fluid velocity. This indicates that the main effect of the interaction (at large Peclét numbers) between the Taylor dispersion mechanism and the shear flow will be a substantial enhancement of solute dispersion in the flow direction.

I.F. is grateful to the Technion V.P.R. Fund – Albert Fund for Research and Development in Aeronautical Engineering. H.B. acknowledges the support of the office of Basic Energy Sciences of the Department of Energy.

REFERENCES

Batchelor, G. K. 1956 On steady laminar flow with closed streamlines at large Reynolds numbers. *J. Fluid Mech.* **1**, 177–190.

Bird, R. B., Armstrong, R. C. & Hassager, O. 1987 *Dynamics of Polymeric Liquids. Vol.* 1: *Fluid Mechanics* 2nd edn. Wiley.

Brenner, H. 1964*a* The Stokes resistance of an arbitrary particle – III Shear fields. *Chem. Engng. Sci.* **19**, 631–651.

Brenner, H. 1964*b* The Stokes resistance of an arbitrary particle – IV Arbitrary fields of flow. *Chem. Engng Sci.* **19**, 703–727.

BRENNER, H. 1967 Coupling between the translational and rotational Brownian motions of rigid particles of arbitrary shape. Part II. General theory. *J. Colloid Interface Sci.* **23**, 407–436.

BRENNER, H. 1972 Suspension rheology. *Prog. Heat Mass Transfer* **5**, 89–129.

BRENNER, H. 1974 Rheology of a dilute suspension of axisymmetric Brownian particles. *Intl J. Multiphase Flow* **1**, 195–341.

BRENNER, H. 1979 Taylor dispersion in systems of sedimenting nonspherical Brownian particles I. Homogeneous, centrosymmetric, axisymmetric particles. *J. Colloid Interface Sci.* **71**, 189–208.

BRENNER, H. 1980 A general theory of Taylor dispersion phenomena. *PhysicoChem. Hydrodyn.* **1**, 91–123.

BRENNER, H. 1982 A general theory of Taylor dispersion phenomena II. An extension. *PhysicoChem. Hydrodyn.* **3**, 139–157.

BRENNER, H. & CONDIFF, D. W. 1972 Transport mechanics in systems of orientable particles III. Arbitrary particles. *J. Colloid Interface Sci.* **41**, 228–274.

BRENNER, H. & CONDIFF, D. W. 1974 Transport mechanics in systems of orientable particles IV. Convective transport. *J. Colloid Interface Sci.* **47**, 199–264.

BURGERS, J. M. 1938 In second report on viscosity and plasticity. *Verhandelingen Koninkl. Ned. Akad. Wetenschap.* **16** (§1, Chap. 3), 113–184.

CERDA, C. M. & VEN, T. G. M. VAN DE 1983 Translational diffusion of axisymmetric particles in shear flow. *J. Colloid Interface Sci.* **93**, 54–62.

DUFTY, J. W. 1984 Diffusion in shear flow. *Phys. Rev.* A **30**, 1465–1476.

ELRICK, D. E. 1962 Source functions for diffusion in uniform shear flow. *Austral. J. Phys.* **15**, 283–288.

FOISTER, R. T. & VEN, T. G. M. VAN DE 1980 Diffusion of Brownian particles in shear flows. *J. Fluid Mech.* **96**, 105–132.

FRANKEL, I. & BRENNER, H. 1991 Generalized Taylor dispersion phenomena in unbounded homogeneous shear flows. *J. Fluid Mech.* **230**, 147–181.

FRANKEL, N. & ACRIVOS, A. 1968 Heat and mass transfer from small spheres and cylinders freely suspended in shear flow. *Phys. Fluids* **11**, 1913–1918.

GIESEKUS, H. 1962 Elasto-viskose Flüssigkeiten, für die in stationären Schichtströmungen sämtliche Normalspannungskompenenten verscheiden grosse sind. *Rheol. Acta* **2**, 50–62.

HESS, S. & RAINWATER, J. C. 1984 Diffusion in laminar flow: Shear rate dependence of correlation functions and of effective transport coefficients. *J. Chem. Phys.* **80**, 1295–1303.

HINCH, E. J. & LEAL, L. G. 1972 The effect of Brownian motion on the rheological properties of a suspension of non-spherical particles. *J. Fluid Mech.* **52**, 683–712.

JEFFERY, G. B. 1922 The motion of ellipsoidal particles immersed in a viscous fluid. *Proc. R. Soc. Lond.* A **102**, 161–179.

KRUSHKAL, E. M. & GALLILY, I. 1984 On the orientation distribution function of nonspherical aerosol particles in a general shear flow I. The laminar case. *J. Colloid Interface Sci.* **99**, 141–152.

LEAL, L. G. & HINCH, E. J. 1971 The effect of weak Brownian rotations on particles in shear flow. *J. Fluid Mech.* **46**, 685–703.

LEIGHTON, D. T. 1989 Diffusion from an initial point distribution in an unbounded simple shear flow. *PhysicoChem. Hydrodyn.* **11**, 377–386.

PETERLIN, A. 1938 Über die Viskosität von verdunnten Lösungen und Suspensionen in Abhangigheit von der Teilchenforme. *Z. Phys.* **111**, 232–263.

SAN MIGUEL, M. & SANCHO, J. M. 1979 Brownian motion in shear flow *Physica* A **99**, 357–364.

SARMAN, S., EVANS, D. J. & CUMMINGS, P. T. 1991 Comment on: Nonequilibrium molecular dynamics calculation of self-diffusion in a non-Newtonian fluid subject to a Couette strain field. *J. Chem. Phys.* **95**, 8675–8676.

SCHERAGA, H. A. 1955 Non-Newtonian viscosity of solutions of ellipsoidal particles. *J. Chem. Phys.* **23**, 1526–1532.

SCHERAGA, H. A., EDSALL, J. T. & GADD, J. O. 1951 Double refraction of flow: numerical evaluation of extinction angle and birefringence as a function of velocity gradient. *J. Chem. Phys.* **19**, 1101–1108.

Stewart, W. E. & Sorensen, J. P. 1972 Hydrodynamic interaction effects in rigid dumbbell suspensions. II. Computations for steady shear flow. *Trans. Soc. Rheol.* **16**, 1–13.

Taylor, G. I. 1953 Dispersion of soluble matter in solvent flowing slowly through a tube. *Proc. R. Soc. Lond.* A **219**, 186–203.